Microscopic Solubility-Parameter Theory of Polymer Blends: General Predictions

Kenneth S. Schweizer* and Chandralekha Singh

Departments of Materials Science & Engineering, Chemistry and Materials Research Laboratory, University of Illinois, Urbana, Illinois 61801

Received November 10, 1994[⊗]

ABSTRACT: A microscopic solubility parameter theory for polymer blends is developed based on liquid-state polymer reference interaction site model (PRISM) integral equation methods. The well-defined approximations to obtain such a description are identified, and tractable schemes to go beyond them are discussed. Analytical predictions for the purely enthalpic χ-parameter are derived using the Gaussian thread model. Many novel, non-Flory–Huggins effects are predicted including the failure of mean-field theory for random copolymer alloys, strong deuteration swap effects, nonadditivity of chemical and conformational asymmetry contributions to the χ-parameter, and unusual and subtle temperature dependences of χ due to thermally-induced density and chain dimension changes. Both general model calculations and applications to specific polyolefins are presented. The simple enthalpy-based theory accounts for the absolute magnitude of olefinic χ-parameters and a wide range of "anomalous" non-Flory–Huggins phenomena observed in recent small-angle neutron scattering and cloud-point experiments. New, experimentally testable predictions are also made. The fundamental origin of the non-mean-field behavior is the dependence of local intermolecular packing, and hence cohesive energy density, on the chain aspect ratio or effective stiffness. Numerical studies using more realistic semiflexible chain models are also presented and are in qualitative agreement with the analytic predictions. The influence of nonlocal, excess entropy of mixing processes is investigated and found to be a relatively small effect for chain aspect ratios characteristic of flexible polymers. Moreover, for blends which can be studied in the miscible phase at experimentally relevant temperatures, the enthalpic contribution to χ arising from conformational asymmetry is generally orders of magnitude larger than the excess entropic contribution. These conclusions provide support for a fundamental assumption of regular solution theory that spatially local enthalpic effects make the dominant contribution to the excess mixture free energy.

I. Introduction

The understanding and prediction of the phase behavior of polymer blends is a challenging theoretical problem of both scientific and commerical importance. Recently, there has been much progress toward constructing microscopic theories based on a variety of different statistical mechanical approaches.[1] A primary goal is to elucidate the influence of polymer structure, intermolecular interactions, and density and concentration correlations on alloy miscibility. In this paper we apply the off-lattice, microscopic liquid-state integral equation approach known as polymer reference interaction site model (PRISM) theory[2,3] to treat this problem at a simplified level which allows contact to be made with more semiempirical approaches. In particular, recent experimental work[4–8] on saturated polyolefin blends has rekindled interest in "regular solution" or "solubility-parameter" ideas[9] which attempt to calculate the mixing properties of blends from a knowledge of the pure-component melt properties or SANS (small-angle neutron scattering) blend-derived component parameters.

One goal of our work is to develop a liquid-state statistical mechanical framework for accessing the validity of regular solution theory and related approaches for polymeric alloys. We are initially interested in using the PRISM methods to construct a melt-based microscopic solubility parameter description which includes the effects of chain architecture, intermolecular forces, and density correlations. Enthalpic interactions (or "cohesive energy density") modified by nonuniversal local chain packing and polymer architecture are assumed to be dominant. The influence of volume changes upon mixing is also briefly investigated. In this paper we establish the general predictions of the PRISM-based melt solubility parameter theory via both analytical analysis and numerical model calculations. Qualitative comparison with blend experimental data is made. In a subsequent companion paper[10] the theory is applied to a wide range of polyolefin and polydiene alloys and its predictions are compared in a detailed manner against experiment. Agreement between the simple theory and experiment is very encouraging, especially for a homologous series of nonpolar alloys. In this and the companion paper we also make novel predictions which can be tested by future, specially-designed experiments and/or computer simulations. Theoretical tests of the underlying approximations of the solubility parameter approach, and the construction of more sophisticated but simplified blend PRISM theories, will be addressed elsewhere.[11]

Before proceeding, we should clearly state our motivation for pursuing more simplified PRISM theories in light of the fact that much previous work has been carried out using the "full" blend theory formulation. There are four basic points. (i) The full PRISM theory, with attractive interactions explicitly accounted for using the new molecular closure schemes, is rather numerically demanding to implement.[15,16,19] (ii) Much general insight can be obtained using the analytically tractable thread model[13,17–20] and the simplified PRISM theories. (iii) Recent experiments suggest a simple solubility parameter approach works surprisingly well for many hydrocarbon alloys.[4–8] (iv) The PRISM theory of *hard-core homopolymer melts* is the only input into our microscopic solubility parameter approach. For this problem the theory has been shown to be very accurate by comparison with both computer simulations[21–23] and experiments.[24,25]

[⊗] Abstract published in *Advance ACS Abstracts,* March 1, 1995.

0024-9297/95/2228-2063$09.00/0

The remainder of this paper is structured as follows. In section II the general liquid-state framework is developed, the approximations which result in a solubility parameter level theory are identified, and more sophisticated theories which relax some of these approximations are outlined. Analytical predictions of the PRISM theory are derived for the Gaussian thread model in section III, and a few illustrative numerical results are presented. Experimentally relevant applications and model calculations based on the thread description are then presented for random copolymer alloys (section IV), the deuteration swap effect (section V), and the temperature dependence of the χ-parameter (section VI). Numerical calculations of the enthalpic and excess entropic contributions to the effective χ-parameter for the less coarse-grained semiflexible chain model are presented in section VII. We summarize and draw conclusions in section VIII. The numerical estimation of solubility parameters for real systems is discussed in the appendix.

II. Microscopic Regular Solution Theory and Beyond

For simplicity we develop the general approach for a binary blend of homopolymers A and B. Each polymer species is taken to consist of a chain of equivalent sites of equal volume (no explicit branching or side groups). We also adopt the Flory-like "ideality" ansatz that the intramolecular structure of the polymers is composition-independent, i.e., the same as in their respective melts.[26] The theoretical liquid-state tools to go beyond this now exist.[27-29]

The blend is characterized by the site number densities, ϱ_A and ϱ_B, the total site number density $\varrho_b = \varrho_A + \varrho_B$, and the composition of the A-species $\phi = \varrho_A/\varrho_b$. The polymer sites on different chains interact via a species-dependent pair potential which consists of repulsive, $u_{MM'}(r)$, and attractive, $v_{MM'}(r) < 0$, branches. For simplicity the repulsive branch is taken to be of a purely hard-core form

$$\begin{aligned} u_{MM'}(r) &= \infty, \quad r \le d_{MM'} \\ &= 0, \quad r > d_{MM'} \end{aligned} \tag{2.1}$$

where $d_{MM'}$ (=d in this work) is the distance of closest approach of sites of type M and M'. These microscopic "hard-core diameters" are temperature-dependent since they mimic the behavior of real continuous, but spatially rapidly varying, repulsive potentials.[30-32]

For the model and conditions described above, the *formally exact* free energy of mixing on a thermal energy basis is:[3,32,33]

$$\beta\Delta F = \left\{\frac{\phi \ln(\phi)}{N_A} + \frac{(1-\phi)\ln(1-\phi)}{N_B}\right\} + \beta F_b^{(0)} + \frac{\beta}{2\varrho_b}\sum_{M,M'} \varrho_M \varrho_{M'} \int d\vec{r}\, v_{MM'}(r) \int_0^1 d\lambda\, g^{\lambda}_{MM'}(r) - \{\phi\beta\,\delta F_{m,A} + (1-\phi)\beta\,\delta F_{m,B}\} \tag{2.2}$$

where N_M is the degree of polymerization of polymer M. The first term is the ideal combinatorial entropy of mixing. The second term is the excess, noncombinatorial free energy of the blend associated with the repulsive interactions and is often referred to as the "excess entropy" (or "athermal") mixture free energy. However, this contribution is generally temperature-dependent for multiple reasons, e.g., a T-dependent hard-core diameter, density, and intramolecular structure. The third term in eq 2.2 is the blend enthalpic contribution, or more precisely the part of the blend free energy associated with the attractive branch of the interchain potential. This contribution takes the form of a "charging" integral from zero attractive potential ($\lambda = 0$) up to the full attractive potential ($\lambda = 1$). In principle, it contains contributions through "infinite order" in inverse temperature due to the possible modification of the interchain site–site pair correlation functions, $g_{MM'}(r)$, by the attractive interactions. The final term is the excess melt free energy contributions, $\delta F_{m,M}$, which are irrelevant if one is only interested (as we are) in the spinodal instability and an effective χ-parameter.

The effective interaction or χ-parameter is defined in terms of the excess blend free energy of mixing, δF_b, as

$$\begin{aligned} \chi &\equiv -\frac{1}{2}\frac{\partial^2 \delta F_b}{\partial \phi^2} \\ &= -\frac{1}{2}\frac{\partial^2}{\partial \phi^2}\left\{\beta F_b^{(0)} + \frac{\beta}{2\varrho_b}\sum_{M,M'} \varrho_M \varrho_{M'} \int d\vec{r}\, v_{MM'}(r) \int_0^1 d\lambda\, g^{\lambda}_{MM'}(r)\right\} \\ &\equiv \chi^{(0)} + \chi_{TH} \end{aligned} \tag{2.3}$$

Thus, χ can be formally separated into its repulsive and attractive force components, often referred to as the "athermal or entropic" and "enthalpic" parts. Calculation of the athermal contribution is discussed in section VII and elsewhere.[34]

Since the basic statistical mechanical approximations of liquid-state integral equation theories are formulated at the level of intermolecular pair correlation functions, not the partition function or free energy, there are several formally equivalent (but in practice inequivalent) routes to calculating thermodynamics.[30,32] We have employed the so-called "free energy route" above. Prior PRISM work has often utilized the so-called "compressibility route" which is formulated in terms of direct correlation functions. Within the framework of the new "molecular closure" approximations,[15-18] separation of the effects of the repulsive and attractive forces at the level of the effective χ-parameter can sometimes be achieved. The issue of the consistency between the two routes has been addressed recently for symmetric[19,33] and structurally asymmetric[34] polymer blends and is discussed further below.

Equations 2.2 and 2.3 provide the starting point for our present work. We now discuss various approximations which result in simplified theories and their connection to phenomenological approaches.

A. Reduction to a Melt Solubility Parameter Description. The simplest Hildebrand, or regular solution, level theory is obtained by invoking the following approximations.

(1) No volume change upon mixing. Thus, the blend number density is composition-independent: $\varrho_b(\phi) \cong \varrho$ = melt density.

(2) The excess repulsive force, or entropic, free energy of mixing is zero. In polymer terms this corresponds to the Flory approximation that only the ideal combinatorial entropy of mixing is important, and hence $\chi^{(0)} \cong 0$.

(3) The intermolecular radial distribution functions in the blend are approximated by their purely repulsive

force values, $g^{\lambda}_{MM'}(r;T) \cong g^{(0)}_{MM'}(r)$. This corresponds to thermodynamic perturbation theory or the so-called "high-temperature approximation" (HTA) for structural correlations.[3,30-32] In a dense melt this is often an excellent approximation, but in mixtures its validity is not obvious. In terms of eqs 2.2 and 2.3, the HTA means the λ-charging integral can be trivially performed.

Invoking approximations (1)–(3) yields a purely enthalpic blend excess free energy

$$\beta\,\delta F_b \cong \frac{\beta}{2\varrho}\sum_{M,M'}\varrho_M\varrho_{M'}\int d\vec{r}\; v_{MM'}(r)\, g^{(0)}_{MM'}(r) \qquad (2.4)$$

To obtain a Hildebrand-like theory requires a final pair of related approximations.

(4a) The diagonal athermal blend correlations, which generally depend on mixture composition ϕ, are approximated by the analogous composition-independent *melt* values $g^{(0)}_{MM}(r;\phi) \cong g^{(0)}_{m,M}(r)$.

(4b) The off-diagonal blend correlations are assumed to obey the "Berthelot" or geometric combining law in terms of the melt correlations

$$-\int d\vec{r}\; v_{AB}(r)\, g^{(0)}_{AB}(r) \cong \{[\int d\vec{r}\; v_{AA}(r)\, g^{(0)}_{m,A}(r)]\,[\int d\vec{r}\; v_{BB}(r)\, g^{(0)}_{m,B}(r)]\}^{1/2} \qquad (2.5)$$

Approximations (1)–(4) then result in a solubility-parameter-like theory with a χ-parameter of purely enthalpic origin

$$\chi_H \cong \frac{1}{2k_BT}([-\varrho\int d\vec{r}\; v_{AA}(r)\, g^{(0)}_{m,A}(r)]^{1/2} - [-\varrho\int d\vec{r}\; v_{BB}(r)\, g^{(0)}_{m,B}(r)]^{1/2})^2 \equiv \frac{1}{2k_BT}(\delta_A - \delta_B)^2 \qquad (2.6)$$

where the subscript "H" denotes a "Hildebrand" approach. In the second line a melt solubility parameter has been defined (in units of square root of cohesive energy) which depends on liquid density, microscopic attractive potentials, and athermal melt radial distribution functions. Note that the chemical interactions between monomers and the interchain structure (packing which depends on chain microstructure and conformation) are *not separable*. The χ-parameter is by definition *independent of blend composition*, which implies the mathematical form of the predicted spinodal and binodal will be identical to the simple mean-field Flory–Huggins behavior. Also note χ must be *nonnegative*. Hence, specific interactions (e.g., hydrogen-bonding, charge transfer), which may result in a negative χ-parameter, cannot be properly described. On the other hand, the χ-parameter can be (weakly) molecular weight dependent and can depend in subtle ways on the nature of the chemical interactions and chain structure and packing of the two components. We also introduce a dimensionless "reduced" solubility parameter

$$\tilde{\delta}_M \equiv \left[\frac{\int d\vec{r}\; v_{MM}(r)\, g^{(0)}_{m,M}(r)}{\int d\vec{r}\; v_{MM}(r)}\right]^{1/2} \qquad (2.7)$$

which contains information about how the local structural correlations deviate from the Flory-like assumption of randomness, i.e., $g(r) = 1$ for $r > d$.

To implement eq 2.6 within PRISM theory requires specification of the melt density, intramolecular structure, and intermolecular potential of the two species. The theory then predicts the radial distribution functions. Applications based on the thoroughly discussed PRISM theory of melts[2,3] are given in sections III–VIII. The spinodal instability condition is given by the standard expression

$$2\chi_H = \frac{1}{\phi N_A} + \frac{1}{(1-\phi)N_B}$$

and the binodal is also easily obtainable.

B. Beyond Simple Hildebrand Theory. The general expression for the effective χ-parameter is given in eq 2.3. Many different theories can be constructed based on relaxing one or more of approximations (1)–(4), which might be thought to result in a "better" theory. The latter statement may not be true in practice since the simple Hildebrand-like theory of eq 2.6 could be accurate due to a cancellation of errors. In this section we enumerate several options which we shall subsequently apply either here or in future publications.

1. "Constant Pressure" Hildebrand Theory. By this we mean relaxing only approximation (1); i.e., the A and B melts have different reduced densities. In the Hildebrand spirit of only using melt information we adopt an ideal combining law for the blend density

$$\varrho_b \cong \phi\varrho_A + (1-\phi)\varrho_B, \qquad \Delta\varrho \equiv \varrho_A - \varrho_B \qquad (2.8)$$

This represents a very crude attempt to account for volume changes upon mixing. Using this approximation, the effective χ-parameter becomes

$$2k_BT\chi = \beta^{-1}\varrho_b^{-1}\frac{\partial^2\varrho_b\beta\Delta F_b}{\partial\phi^2} = (\delta_A - \delta_B)^2 - 4\frac{\Delta\varrho}{\varrho_b}(\delta_A - \delta_B)\delta_{AV} + \left(\frac{\Delta\varrho}{\varrho_b}\right)^2\delta_{AV}^2 \qquad (2.9a)$$

where δ_{AV} is an average solubility parameter

$$\delta_{AV} \equiv \phi\delta_A + (1-\phi)\delta_B \qquad (2.9b)$$

The solubility parameters in the above equations are defined as in eq 2.6 *but* with ϱ replaced by ϱ_b of eq 2.8. Equation 2.9a can be written in a more revealing form by factoring out the constant density contribution

$$\chi = \frac{(\delta_A - \delta_B)^2}{2k_BT}\{1 - 2\Psi + (\Psi/2)^2\} = \frac{(\Delta\delta)^2}{2k_BT}\{(1-\Psi/2)^2 - \Psi\} = \chi_H\{(1-\Psi/2)^2 - \Psi\} \qquad (2.10)$$

where

$$\Psi \equiv \frac{\Delta\varrho}{\varrho_b}\frac{\delta_A + \delta_B}{\delta_A - \delta_B} = 2\frac{\Delta\varrho}{\varrho_b}\frac{\delta_{AV}}{\Delta\delta}, \qquad \Delta\delta \equiv \delta_A - \delta_B \qquad (2.11a)$$

Note there are two (weakly) composition-dependent contributions associated with the differences in melt densities. However, their net effect is contained in the parameter Ψ, and a variety of behaviors are possible including a *negative* χ-parameter. For polymer blends the new terms are not obviously negligible, even if $\Delta\varrho/\varrho_b$ is of order 0.01 or less, since typical melt solubility parameter differences of miscible systems are small.

This point is perhaps made clearer by rewriting eq 2.11a as

$$\Psi = 2\frac{\Delta\varrho}{\varrho_b}\frac{\phi(-\beta U_A)^{1/2} + (1-\phi)(-\beta U_B)^{1/2}}{(2\chi_H)^{1/2}} \quad (2.11b)$$

where U_M is the cohesive energy of species M.

2. Blend Hildebrand Theories. The simplest case corresponds to relaxing only approximation (4a), but the geometric combining law of eq 2.5 is still retained *using blend information*. Moreover, when carrying out the second derivative of the free energy of mixing, we *assume that derivatives of the radial distributions are negligible*, which is in the Hildebrand spirit. The result is a χ-parameter precisely of the form of eq 2.6, but the solubility parameters are now in terms of the athermal blend structure.

$$\delta_M \equiv [-\varrho\int d\vec{r}\; v_{MM}(r)\, g^{(0)}_{MM}(r;\phi)]^{1/2} \quad (2.12)$$

Although the corresponding χ-parameter remains nonnegative, it will in general be composition-dependent. The motivation for considering this case is that it corresponds to the successful recent experimental analysis of polyolefin mixing in terms of the regular solution framework but with *solubility parameters derived from blend (not melt) data*.[4-8]

An alternative approach, which still assumes the dominance of the constant volume enthalpic contribution, corresponds to relaxing both approximations (4a) and (4b). If one still assumes that when carrying out the second derivative of the free energy of mixing the *derivatives of the radial distributions are negligible*, the result is

$$\chi \cong \frac{\varrho}{2k_BT}\int d\vec{r}\; \{-v_{AA}(r)\, g^{(0)}_{AA}(r) - v_{BB}(r)\, g^{(0)}_{BB}(r) + 2v_{AB}(r)\, g^{(0)}_{AB}(r)\} \quad (2.13)$$

This χ-parameter is of the form of an "exchange" energy à la Flory theory, but with the athermal blend correlations not all equal to unity.

Complete relaxation of approximation (4) implies

$$\chi \cong -\frac{\varrho}{2k_BT}\frac{\partial^2}{\partial\phi^2}\int d\vec{r}\; \{\phi^2 v_{AA}(r)\, g^{(0)}_{AA}(r) + (1-\phi)^2 v_{BB}(r)\, g^{(0)}_{BB}(r) + 2\phi(1-\phi)v_{AB}(r)\, g^{(0)}_{AB}(r)\} \quad (2.14)$$

which fully accounts for contributions to χ due to possible ϕ-dependence of the blend pair correlations. Numerical investigation of all these "blend Hildebrand" approaches will be presented elsewhere.[11]

3. More Sophisticated Approaches. Obviously there are a large number of additional possibilities which involve relaxing more of the approximations (1)–(4). All these can be investigated using PRISM theory. The reliability of approximation (2) has already been investigated for short chain, hard-core, conformationally asymmetric blends using Monte Carlo simulations and PRISM theory.[34b] The computed athermal χ-parameters were found to be very small consistent with the Flory-like assumption of a negligible excess entropy of mixing. A similar conclusion has been reached using PRISM theory for conformationally asymmetric *high* molecular weight blends and diblock copolymers composed of chains of aspect ratios relevant to most experimental flexible polymers.[34a] These conclusions are very different from those deduced using incompressible field theories of Gaussian chain alloys which emphasize nonlocal excess entropic effects.[35]

III. Analytic Thread PRISM Theory of Melt Solubility and Enthalpic χ-Parameters

In this section analytical expressions are derived for the melt solubility parameters and a Hildebrand-like χ-parameter using the simplified Gaussian thread model and hard-core (athermal) melt PRISM theory. All the thread melt results required have been previously discussed.[3,20,27,36] We note in passing that this model can be employed as an effective one-component description of polymer solutions. Connections between the thread PRISM predictions and field theoretic[37] and blob scaling[26] approaches for the pair correlations, screening length, and osmotic pressure are derived elsewhere.[20,27,36]

A. Melt Properties. The thread model represents a polymer chain as an infinitely thin Gaussian space curve ($d \to 0$) which occupies a finite volume fraction of space and satisfies a pointlike hard-core constraint: $g(r=0) = 0$. When combined with the PRISM integral equation, the latter condition results in a nontrivial result for the chain-averaged intermolecular site–site radial distribution function and density–density total structure factor $\hat{S}(k)$:

$$g_0(r) = 1 + \frac{3\sigma}{\pi\varrho\sigma^3 r}[\exp(-r/\xi_\varrho) - \exp(-r/\xi_C)] \quad (3.1)$$

$$\hat{S}(k) = \frac{12\xi_\varrho^{\,2}}{1 + k^2\xi_\varrho^{\,2}} \quad (3.2)$$

where the correlation lengths are given by

$$\xi_\varrho^{\,-1} = \frac{\pi}{3}\varrho\sigma^3 + \xi_C^{\,-1}, \qquad \xi_C = \frac{R_g}{2\sigma} = \left(\frac{N}{12}\right)^{1/2} \quad (3.3)$$

Here, N is the number of segments, σ the statistical segment length, and the correlation lengths are written in dimensionless form in units of σ. The athermal $g_0(r)$ contains a "local" contribution from density fluctuations via the screening length ξ_ϱ, and a universal "long-range correlation hole" contribution associated with the length scale ξ_C. Interaction strength in the compressible hard-core fluid is characterized by the dimensionless segmental number density $\varrho\sigma^3$. Hence, the density–density screening or correlation length depends on the chain stiffness and controls the depth of the *local* correlation hole.

Contact with an incompressible RPA-like approach corresponds to setting the density screening length to zero but retaining a finite chain length polymer. In this case there still is a "correlation hole", but it is of universal "global" origin. We shall never invoke such a locally unrealistic approximation, which has been shown to be particularly suspect for structurally asymmetric alloys.[18]

The (osmotic) compressibility is proportional to the collective structure factor at $k = 0$:

$$\hat{S}(0) = 12\xi_\varrho^{\,2} = \frac{108}{\pi^2}(\varrho\sigma^3)^{-2}, \qquad \text{as } N \to \infty \quad (3.4)$$

Hence, the repulsive force compressibility decreases as the statistical segment length density increases. For analytical convenience, the attractive site–site interac-

tions are modeled as a screened Coulomb form

$$v_M(r) = -\epsilon_M \frac{\exp(-r/a_M)}{r/a_M}, \quad \epsilon_M > 0 \qquad (3.5)$$

where a_M is the spatial range and ϵ_M is the energy parameter for species M. The connection between the thread potential parameters and those of real hydrocarbon molecules is discussed in the appendix.

Within the HTA approach, the cohesive energy density per segment (of volume V_M) is

$$\frac{U_{COH,M}}{V_M} \equiv \frac{\varrho_M^2}{2}\int d\vec{r}\; v_M(r)\, g_{0,M}(r) \qquad (3.6)$$

$$= -2\pi\epsilon_M\varrho_M^2 a_M^3\left\{1 - \frac{3\sigma_M}{\pi a_M}(\varrho_M\sigma_M^3)^{-1}\left[\frac{1}{1+(a_M/\xi_C)} - \frac{1}{1+(a_M/\xi_\varrho)}\right]\right\} \qquad (3.7)$$

The corresponding solubility and reduced solubility parameters of eqs 2.6 and 2.7 are given by

$$\delta_M = (2\pi\epsilon_M\varrho_M^2 a_M^3)^{1/2}\,\tilde{\delta}_M \qquad (3.8)$$

$$\tilde{\delta}_M = \sqrt{\left\{1 - \frac{3\sigma_M}{\pi a_M}(\varrho_M\sigma_M^3)^{-1}\left[\frac{1}{1+(a_M/\xi_C)} - \frac{1}{1+(a_M/\xi_\varrho)}\right]\right\}} \qquad (3.9)$$

Examination of these expressions shows that the solubility parameter is predicted (at constant volume) to *decrease weakly with N*. This is a finite size effect which arises from the interference between the local density screening and long-range correlation hole length scales. Some experimental evidence for this trend exists for polystyrene[38] and poly(ethylenepropylene) (PEP)[39] oligomer melts. Note also that in the *literal* incompressible limit ($\varrho \to \infty$) the reduced solubility parameter reduces to its trivial mean-field value of unity.

In the large N limit, $\xi_\varrho/\xi_C \to 0$ and the reduced solubility parameter simplifies to

$$\tilde{\delta} = \frac{1}{\left(1 + \frac{3}{\pi\varrho\sigma^2 a}\right)^{1/2}} = \frac{1}{\left(1 + \xi_\varrho\frac{\sigma}{a}\right)^{1/2}} \qquad (3.10)$$

The relevant dimensionless density involves all three local nonuniversal length scales: the density screening length, the attractive potential range, and the statistical segment length. For a *fixed* attractive potential range, this relation predicts that *for thread melts* the only relevant quantity is the *statistical segment length squared per unit volume*, $\varrho\sigma^2$, which is invariant to the redefinition of the segment length by regrouping of real monomers (see Table 1). The importance of such an invariant quantity in blends of conformationally asymmetric polymers has been recently emphasized by Bates and co-workers[40] in the context of quasi-universal unfavorable *excess entropy* of mixing.[35] Here, this "segment length on an equal volume basis" quantity arises rigorously from the *thread melt* PRISM theory for the *enthalpic* solubility parameter.[36]

Table 1. Calculated Invariant Parameter (in Angstroms) and Effective Aspect Ratio Based on Averaged Literature Data for T = 430 K Polymer Properties and a Reference Volume of 90 Å^3 (See Reference 36)

polymer	$(\varrho\sigma^2)^{-1}$	Γ
polyethylene (PE)	2.0	1.21
poly(ethylenepropylene) (PEP)	2.8	1.01
polyisobutylene (PIB)	3.69	0.88
polypropylene (PP)	3.33	0.93
a-poly(ethylethylene) (PEE)	5.0	0.76
a-polystyrene (PS)	3.84	0.87
1,4-polybutadiene (PBD)	2.33	1.12
1,4-polyisoprene (PI)	2.93	1.0
1,2-polybutadiene (PVE)	3.49	0.91
a-poly(methyl methacrylate) (PMMA)[a]	4.43	0.81
poly(tetrafluoroethylene) (PTFE)[b]	1.47	1.41

[a] Based on a density of 1.18 g/cm^3 and a characteristic ratio of 7. [b] Based on a density of 2 g/cm^3 and a 430 K characteristic ratio of 12.5.[58]

The reduced solubility parameter is predicted to increase as the chain stiffness on an equal volume basis increases. This conclusion has also been reached using more realistic single-chain models[36,41] and appears to be model-independent. Equation 3.10 also predicts that as the attractive potential becomes spatially longer range the reduced solubility parameter will increase since the shallower region of the local correlation hole is sampled more heavily (i.e., $g_0(r) = 1$ is a better approximation). Numerical estimation of the reduced solubility parameter for real systems is discussed in the appendix.

It is instructive to rewrite eq 3.10 in two additional forms. Defining the melt packing fraction as $\eta = \pi\varrho d^3/6$ and the aspect ratio as $\Gamma = \sigma/d$ and using eqs 3.3 and 3.4 yields

$$\tilde{\delta} = \frac{1}{\left(1 + \frac{d/a}{2\eta\Gamma^2}\right)^{1/2}} \qquad (3.11)$$

$$\tilde{\delta} = \frac{1}{\left(1 + \frac{\sigma}{a}\left(\frac{\hat{S}_0(0)}{12}\right)^{1/2}\right)^{1/2}} \qquad (3.12)$$

In these forms it is clear that the reduced solubility parameter is predicted to decrease as the liquid becomes more compressible (see eq 2.5) or as the aspect ratio on an equal segment diameter basis decreases. Such structure–property correlations are *globally* supported by recent SANS and *PVT* measurements on polyolefins.[4,6,8]

B. Constant Volume Predictions for χ. Each species of the constant volume thread blend is characterized by its statistical segment length σ_M, number of segments N_M, attractive Yukawa potential range and strength a_M and ϵ_M, and common segmental number density ϱ. We introduce the ratio variables[18]

$$\gamma \equiv \frac{\sigma_B}{\sigma_A} = \frac{\Gamma_B}{\Gamma_A}, \quad \lambda^2 \equiv \frac{\epsilon_B}{\epsilon_A}\left(\frac{a_B}{a_A}\right)^3 \qquad (3.13)$$

which characterize the conformational (on an equal volume basis) and interaction potential asymmetries. Based on the Hildebrand form of eq 2.6, the predicted χ-parameter in the *long-chain* limit is

$$\chi_H = \frac{1}{2k_BT}(\delta_B - \delta_A)^2 \qquad (3.14)$$

$$\delta_M = \frac{(4\pi a_M^3 \varrho \epsilon_M)^{1/2}}{\left(1 + \frac{3}{\pi \varrho \sigma_M^2 a_M}\right)^{1/2}} = \frac{(4\pi a_M^3 \varrho \epsilon_M)^{1/2}}{\left(1 + \frac{1}{2\eta \Delta_M \Gamma_M^2}\right)^{1/2}} \quad (3.15)$$

where the solubility parameter has been written in two alternative, but equivalent, forms. Here, $\Delta_M = a_M/d$ is a potential range ratio, and $\Gamma_M = \sigma_M/d$ is an aspect ratio of species M. Small corrections for finite chain lengths can be incorporated using eq 3.9, and result in a molecular weight dependence of the χ-parameter which may be significant for oligomers.

For simplicity, and in the spirit of the equal segmental volume mapping implicit to the thread model, we adopt a common attractive potential range a. Equation 3.14 can then be written as

$$\chi_H = 6\beta\eta\Delta^3(\epsilon_B\epsilon_A)^{1/2}\left(\frac{\lambda^{1/2}}{\left(1 + \frac{1}{2\eta\Delta\Gamma_B^2}\right)^{1/2}} - \frac{\lambda^{-1/2}}{\left(1 + \frac{1}{2\eta\Delta\Gamma_A^2}\right)^{1/2}}\right)^2 \quad (3.16)$$

In this form one immediately sees the "competition" between the chemical interaction and conformational (aspect ratio) asymmetries in determining χ and the possibility of "asymmetry cancellation".[18] If the conformational and chemical asymmetries are comparable, then they do not enter the χ-parameter in an additive manner, i.e., the "cross-term" is always important. The dependence of the enthalpic χ on the effective aspect ratio enters in a nonanalytic manner via its influence on the local density screening length in the melt. In the "structurally symmetric" limit corresponding to equal aspect ratios, eq 3.16 reduces to a simpler form where $\chi_H \propto \epsilon_A(\lambda - 1)^2$ as in Flory–Huggins theory.

One also sees from eq 3.16 that the consequence of deuteration of one of the species depends on which hydrogenated polymer has the larger solubility parameter. Since complete deuteration effectively lowers ϵ_M by roughly a few percent, then the χ-parameter generally increases (decreases) if the smaller (larger) solubility parameter species is labeled. Such a "swap" effect has been experimentally observed in binary blends of ethylene–butene-1 (PE–PEE) random copolymers at both the SANS-derived χ-parameter level and via direct cloud-point measurements.[4,5,42,43]

As discussed in the appendix and elsewhere,[36,40] estimates of the invariant parameter $\varrho\sigma^2$ for polyolefins and polydienes yield typical values in the range $0.2 < \varrho\sigma^2 < 0.5$ (see Table 1). Hence, from eq 3.11, a reasonable (but *unnecessary*) mathematical simplification of the square root factor in eq 3.16 yields

$$\chi_H \approx \frac{6\eta\Delta^3}{k_BT}(\epsilon_A\epsilon_B)^{1/2}\left(\sqrt{\lambda} - \frac{1}{\sqrt{\lambda}} - \frac{1}{4\eta\Delta}\left\{\frac{\sqrt{\lambda}}{\Gamma_B^2} - \frac{1}{\sqrt{\lambda}\,\Gamma_A^2}\right\}\right)^2 \quad (3.17)$$

For idealized "chemically symmetric" blends $\lambda = 1$, and the "bare" Flory–Huggins χ-parameter is *zero*. For this "effectively athermal" situation, eq 3.17 simplifies to

$$\chi_H \approx \frac{3\Delta\epsilon}{8\eta\Gamma_B^4 k_BT}(\gamma^2 - 1)^2 \quad (3.18)$$

In this limit the χ-parameter is predicted to grow with increasing stiffness asymmetry according to the factor $(\gamma^2 - 1)^2$, a result previously obtained from analytic *blend* PRISM theory based on the *compressibility route* to the thermodynamics.[18] This simple dependence has also been derived for *athermal* conformationally asymmetric blends using incompressible field theory.[35] However, this is a mathematical similarity only since our result is of purely enthalpic, local origin, not of nonlocal excess entropic origin. Equation 3.18 also predicts that structural asymmetry is less important as the B-chain aspect ratio increases, i.e., as the average aspect ratio of the blend gets larger.

Finally, note that, in the *hypothetical incompressible limit* ($\eta \to \infty$ corresponding to zero density fluctuations), the above χ-parameter for this $\lambda = 1$ case is *identically zero*, i.e., the mean-field bare value. Thus, the incompressibility approximation represents an unphysical limiting case for the local enthalpic χ-parameter.

C. Absolute Magnitudes and Asymmetry Competition. Consider the absolute magnitude of the predicted χ-parameter for polyolefin alloys. On the basis of eqs A1–A3, on a *single* methylene group basis, one obtains

$$\chi_H \cong \frac{600}{T}\left(\frac{1}{\left(1 + \frac{0.176}{\varrho_B\sigma_B^2}\right)^{1/2}} - \frac{1}{\left(1 + \frac{0.176}{\varrho_A\sigma_A^2}\right)^{1/2}}\right)^2 \quad (3.19)$$

In this equation we have assumed (for simplicity) the bare χ-parameter is *zero*, *i.e.*, $\lambda = 1$. Although never literally true, this assumption may be a reasonable approximation for molecules such as the polyolefins.

Using this equation, one can estimate the absolute magnitude of χ for typical polyolefin homopolymer blends. Values of the invariant quantity $\varrho\sigma^2$ are listed in Table 1. The chain aspect ratio is calculated using eq A4 based on a common reference volume, V_{ref}, of 90 Å^3 as:[36]

$$\Gamma_{ref} \equiv \left(\frac{\pi}{6V_{ref}}\right)^{1/3}\left(\frac{6R_g^2}{N_{mon}}\frac{V_{ref}}{V_{mon}}\right)^{1/2} \quad (3.20)$$

As expected physically, the aspect ratios are of order unity.

Using the above results yields the following 430 K values for χ of the A/B blend pair on a *four carbon* basis: 0.0096 (PE/PEP), 0.095 (PE/PEE), and 0.044 (PEP/PEE). The experimental estimates by Graessley et al. are[6] 0.005 (PE/PEP), 0.045 (PE/PEE), and 0.014 (PEP/PEE) at 430 K. The relative ordering of χ for the three cases is correctly predicted. Moreover, there appears to be absolute magnitude agreement to within a factor of roughly 3. This may be fortuitous but is encouraging with regards to the usefulness of a microscopic solubility parameter approach and the idea that thermodynamic incompatibility is dominated by enthalpic effects modified by the influence of conformational asymmetry on local packing.

One of the most interesting predictions of eqs 3.14–3.16 is the possibility of "compensation" of the conformational and chemical interaction asymmetries to produce a small enthalpic χ-parameter.[18] If one can form miscible blends composed of structurally and interaction asymmetric polymers, then such alloys would most likely have novel material properties. Of

course, an important caveat is that if the reduced densities of the two components are significantly different, then strong modification of any constant volume estimates may occur. In Figure 2 we present sample calculations of χ for several values of the asymmetry parameters. The calculations are based on eq A5:

$$\tilde{\delta}_B = \frac{\lambda}{\left(1 + \frac{0.515}{\Gamma_B^2}\right)^{1/2}}, \qquad \tilde{\delta}_A = \frac{1}{\left(1 + \frac{0.515}{\Gamma_A^2}\right)^{1/2}} \tag{3.21}$$

The results are purely illustrative but do employ realistic melt estimates of the required factors. The crossing of the curves, and the change in the sign of the slope, indicates the nonadditivity of conformational and chemical interaction asymmetries in determining the enthalpic χ-parameter.

The question of whether the structural and chemical asymmetries tend to "compensate" or "reinforce" depends on the absolute *and* relative values of the asymmetry ratios $\gamma = \Gamma_B/\Gamma_A$ and $\lambda = (\epsilon_{BB}/\epsilon_{AA})^{1/2}$. For the polyolefins, one expects (on an equal volume basis) the effective stiffness and chemical interaction strength to *both decrease* as more methylene groups are replaced by methyl and CH units via side-group substitution; i.e., γ and λ are both greater than 1 if we use the convention that the A-polymer is the more branched. A similar situation is expected for the polydienes; e.g., polybutadiene is "stiffer" (on an equal volume basis) and more strongly interacting than polyisoprene which has a hydrogen atom replaced by a methyl group. Hence, for these two cases the asymmetries tend to reinforce and promote phase separation, although selective deuteration can lead to subtleties.

On the other hand, a blend of polyethylene and polybutadiene might correspond to the compensation situation since the saturated PE is conformationally stiffer but the polydiene is a chemically stronger interacter due to the more polarizable carbon double bond. [However, destabilizing equation-of-state effects due to volume differences are probably very significant.] A similiar situation applies to polyethylene and Teflon (poly(tetrafluoroethylene), PTFE). Assuming crystallization is not an issue (which it no doubt is), then since Teflon is the conformationally stiffer chain but interacts more weakly due to fluorination, the compensation case should apply. More practically, this case would be relevant to random copolymer alloys composed of PE and PTFE units or poly(vinylidene fluoride) (PVF2). The magnitude of any compensation or reinforcement depends, of course, on the chemical and structural details of the specific polymer pair.

D. Effect of Volume Changes on χ. Within our simple approach, the effect of mixing volume changes on χ is given by eq 2.9 or 2.10 combined with eq 3.15. There are three general cases depending on the sign and magnitude of the parameter Ψ of eq 2.11. (1) $\Psi < 0$ or $\Psi > 8$ which results in destabilization of the blend relative to the constant volume case (i.e., increase of χ). (2) $0 < \Psi < 4 - 2\sqrt{3}$ or $4 + 2\sqrt{3} < \Psi < 8$ which results in a positive χ but smaller than the constant volume case, i.e., stabilization of the blend. (3) $4 - 2\sqrt{3} < \Psi < 4 + 2\sqrt{3}$ results in a *negative* χ. The general behavior is illustrated in Figure 1. As an important caveat, the question of whether the origin of negative χ-parameters in nonpolar hydrocarbon alloys,[8,44] or other "unusual" features, are due to volume changes is not obvious.

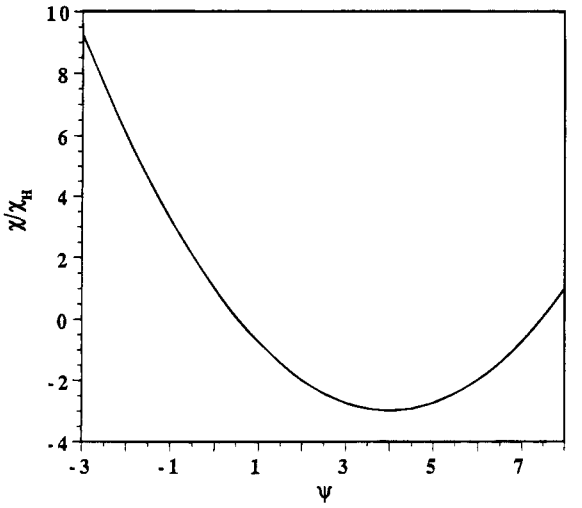

Figure 1. Ratio of the "constant pressure" Hildebrand χ-parameter to its constant volume analog as a function of the dimensionless variable Ψ. The constant volume case corresponds to a ratio of unity and $\Psi = 0$.

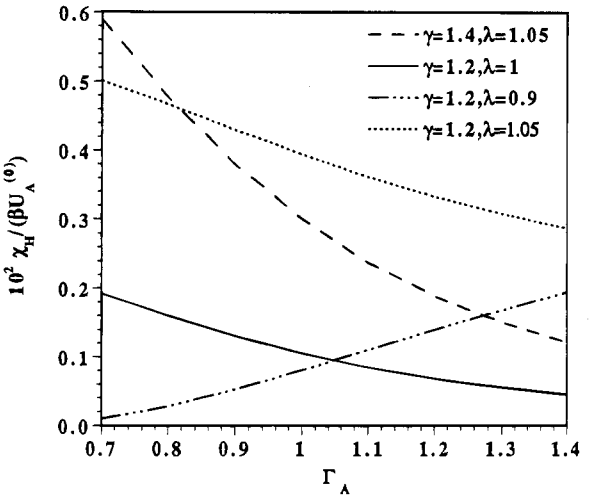

Figure 2. χ-parameter scaled by the mean-field cohesive energy of species A in thermal units versus the A-chain aspect ratio for several values of the conformational and chemical interaction asymmetry variables.

Alternative mechanisms, such as "specific packing" effects between branched molecules, may be important.

The magnitude of the terms associated with the density differences may be comparable to the leading order positive constant volume contribution. We illustrate this in Table 2 where experimental *PVT*-derived melt solubility parameters and densities of a variety of polyolefins have been employed to crudely estimate the reduced difference quantities and hence Ψ. (The reduced densities are estimated using 23 °C data, but these values are a good approximation to the 167 °C values if the thermal expansion coefficients of the different melts are nearly the same, as they are for most polyolefins.) As expected, no universal behavior is found, and all three subcases enumerated above seem possible even within a simple class of materials such as the polyolefins.

There are a number of interesting consequences of our simple model of the effect of volume changes. "Irregular" mixing,[6,8] as characterized by positive or negative deviations from the constant volume prediction, is possible. For example, based on the estimated parameters, one sees from Table 2 that a large stabilization (relative to the constant volume case) of the PP/hhPP

Table 2. Reduced Density (at T = 23 °C[4-8,49]) and Solubility Parameter (at T = 167 °C[4-8]) Differences Based on Experimental Melt Data[a]

A/B[b]	$10^3\Delta\varrho/\varrho_{av}$	$10^3\Delta\delta/\delta_{av}$	Ψ	χ/χ_H
dPEE/hPEE	1.9	≅−[10,20]	[−0.4,−0.2]	[1.8,1.4]
dPVE/hPVE	3.9	≅−[10,20]	[−0.8,−0.4]	[2.8,1.8]
PEP/PE	≅0	54.1	≅0	≅1
PEP/PEE	−17.9	66.7	−0.54	2.1
PE/PEE	−17.9	121	−0.30	1.6
PP/hhPP	−11.2	−49.8	0.45	0.15
PEP/hhPP	−21.5	3.6	−12.0	37.0
PP/PEP	10.4	−53.4	−0.39	1.8
PP/PEB	−0.8	−49.8	0.03	0.94
PEP/PEB	−11.1	−37.2	0.6	−0.1
PIB/PEB	69.7	41.1	3.4	−2.9
EB97/88	1.85	−22.4	−0.17	1.34

[a] The calculated parameter Ψ is also listed, as is the ratio of the predicted χ-parameter which includes the density change to its constant volume analog (see eq 2.10). Two estimates are shown for isotopic blends which span the range estimated in ref 49. Recent *PVT*-based solubility parameter measurements[8] on EB8 ethylene/butene random copolymer melts yield a smaller value of $\Delta\delta/\delta_{av} \cong -6 \times 10^{-3}$ corresponding to a chemical asymmetry parameter of $\lambda \cong 1.006$. [b] EBy = random copolymers of PE and PEE monomers of y% PEE monomers. hhPP = head-to-head polypropylene. PEB = poly(ethylenebutene).

blend, and a negative χ-parameter for the PIB/PEB blend, are suggested. These behaviors appear to be in qualitative agreement with experiments.[8] On the other hand, a large destabilization of the PEP/hhPP blend relative to the constant volume estimates is suggested which does not seem to be the case experimentally.[8] Clearly, these estimates are very sensitive to the small difference quantities required.

Since the temperature dependence of the melt solubility parameters and densities are variable and system-specific, the key parameter Ψ in eq 2.11 may also display unusual temperature dependences which can *counteract or reinforce* the temperature dependence of the constant volume contribution to χ in eq 2.6 or 3.14. As a result, subtle and complex thermal responses may be observed for the net χ. Finally we note that even if the melt solubility parameters are matched, and hence $\Delta\delta = 0$ in eq 2.10, the χ-parameter is nonzero

$$\chi = \frac{\beta}{2}\left(\frac{\Delta\varrho}{\varrho_b}\right)^2 \delta_{AV}^2, \quad \text{if } \Delta\delta \to 0 \tag{3.22}$$

and is potentially of significant magnitude since $\beta\delta_{AV}^2/2 \cong 1$ for a typical hydrocarbon polymer.

In the next three sections we present additional algebraic analysis and model calculations based on the results of this section using the constant volume approach. Our purpose is to more explicitly display the predictions which might be experimentally tested. The results presented are primarily motivated by recent measurements on polyolefin alloys but apply more generally. Applications to specific polyolefin and polydiene blends, and detailed comparison with experiments, will be presented in our future companion paper.[10]

IV. Random Copolymer Blends

A random AB copolymer consists of chemically distinct monomers A and B bonded together in the same chain. The copolymer composition, y, denotes the fraction of the molecule which is A monomer. Binary blends of random AB copolymers of the *same* A and B monomers, but of different compositions y_A and y_B, often form miscible alloys. According to Flory–Huggins mean-field theory, the enthalpic χ-parameter of such a random copolymer blend is[45]

$$\chi_{FH} = (y_B - y_A)^2 \chi^{(0)}_{blend} \equiv (\Delta y)^2 \chi^{(0)}_{blend} \tag{4.1}$$

where $\chi^{(0)}_{blend}$ is the Flory–Huggins χ-parameter of the blend of A and B homopolymers which for our analytic thread model is given by

$$\chi^{(0)}_{blend} = 2\pi\beta|\epsilon_{AA}|\varrho a^3(\lambda - 1)^2 \tag{4.2}$$

Note that the ratio $\chi_{FH}/(\Delta y)^2$ is predicted to be a constant, independent of the precise values of y_A and y_B.

Within thread PRISM theory at the solubility parameter level, the above mean-field result follows from assuming random mixing ($g(r) = 1$ for $r > d$) and adopting an "effective homopolymer" description of the random copolymer in the sense that the cohesive energy is given by

$$\begin{aligned} -U_{COH} &= 4\pi\varrho a^3(y^2\epsilon_{AA} + (1-y)^2\epsilon_{BB} + 2y(1-y)\epsilon_{AB}) \\ &= 4\pi\varrho a^3(y\epsilon_{AA}^{1/2} + (1-y)\epsilon_{BB}^{1/2})^2 \end{aligned} \tag{4.3}$$

Here the geometric combining law for the AB energy parameter has been employed ($\epsilon_{AB} = [\epsilon_{AA}\epsilon_{BB}]^{1/2}$). Use of eq 4.3 in the blend enthalpy expression of eq 2.4, in conjunction with the Hildebrand and random mixing approximations, yields the Flory–Huggins result of eq 4.1.

Recent experiments on blends of polyolefin random copolymers have found large deviations from the mean-field prediction in the sense that the effective χ-parameter also depends strongly on the *average* copolymer composition.[4,6] Within thread PRISM, this is understandable if the effective segment length depends on copolymer composition, y. Using the same effective homopolymer model and Berthelot approximation for the AB energy parameter discussed above, a Hildebrand χ-parameter of the form of eq 3.14 is obtained with a solubility parameter of

$$\delta_M = \frac{(4\pi\varrho a^3)^{1/2}\{y\epsilon_{AA}^{1/2} + (1-y)\epsilon_{BB}^{1/2}\}}{\left(1 + \frac{3}{\pi\varrho\sigma_M^2(y)a}\right)^{1/2}} = \frac{(4\pi\varrho a^3\epsilon_{AA})^{1/2}\{y + (1-y)\lambda\}}{\left(1 + \frac{1}{2\eta\Delta\Gamma_M^2(y)}\right)^{1/2}} \tag{4.4}$$

where $\Delta = a/d$. The presence of conformational asymmetry destroys the simple mean-field relation $\chi \propto (\Delta y)^2$.

The nature and magnitude of the deviations from the mean-field Flory behavior depend sensitively on non-universal system parameters. A general qualitative feeling for the deviations can be obtained by considering the following hypothetical experiment. Imagine the compositional *difference* is extremely small, i.e., $\Delta y \to 0$, and measure the dependence of the χ-parameter on the *average* composition variable defined as y. Using the first form of eq 4.4 and eq 3.14, one obtains

$$\frac{\chi_H}{(\Delta y)^2} \propto \frac{1}{1+\frac{3}{\pi\rho a\sigma^2(y)}}\left\{(\lambda-1)+\frac{3}{2\pi}(y+\lambda(1-y))\times \frac{(\Delta\sigma^2/\rho a\sigma^4(y))}{1+\frac{3}{\pi\rho a\sigma^2(y)}}\right\}^2 \quad (4.5)$$

where the effective segment length squared of an AB random copolymer has been estimated in a Gaussian manner as

$$\rho\sigma^2(y) = y\rho\sigma_A{}^2 + (1-y)\rho\sigma_B{}^2$$

$$\Delta\sigma^2 \equiv \sigma_B{}^2 - \sigma_A{}^2 \quad (4.6)$$

Equation 4.6 is a preaveraging approximation which treats the random copolymer as an effective homopolymer with a composition-dependent statistical segment length. The same approximation was employed for the effective energetic interaction in eqs 4.3 and 4.4. We expect such a simple treatment is reasonable for a purely random sequence distribution and possibly also a regular alternating AB sequence. For "blocky" sequence distributions this effective medium approximation is probably unreliable, especially if microphase separation is a possibility.

Now, a measure of the overall deviation from Flory theory is the ratio of the χ-parameter of eq 4.5 in the limiting $y = 0$ and $y = 1$ average composition cases. This ratio is given by

$$\frac{\chi_H(y=1)}{\chi_H(y=0)} = \left(\frac{1+\frac{3}{\pi\rho a\sigma_B{}^2}}{1+\frac{3}{\pi\rho a\sigma_A{}^2}}\right)\times \left\{\frac{(\lambda-1)+\frac{3\Delta\sigma^2}{2\pi\rho a\sigma_A{}^4}\left(1+\frac{3}{\pi\rho a\sigma_A{}^2}\right)^{-1}}{(\lambda-1)+\lambda\frac{3\Delta\sigma^2}{2\pi\rho a\sigma_B{}^4}\left(1+\frac{3}{\pi\rho a\sigma_B{}^2}\right)^{-1}}\right\}^2, \quad \Delta y \to 0 \quad (4.7)$$

Note that if the A and B segment lengths are the same, or the literal incompressible limit is enforced, then eq 4.7 reduces to 1, i.e., the Flory result. The leading factor in the above equation is the square of the ratio of reduced solubility parameters and hence for a miscible system is not expected to deviate from unity very much. On the other hand, the second factor can deviate from unity by a small or large amount depending on the specific system. A general feature is that, as the chemical asymmetry becomes larger (big $|\lambda - 1|$) and/or the conformational asymmetry becomes smaller, deviations from the y-independent Flory prediction become *smaller*. Again, the precise behavior depends on whether the chemical and conformational asymmetries tend to compensate or reinforce.

For perfect chemical interaction symmetry, $\lambda = 1$, eq 4.7 simplifies to

$$\frac{\chi_H(y=1)}{\chi_H(y=0)} = \gamma^8\left(\frac{1+\frac{3}{\pi\rho a\sigma_B{}^2}}{1+\frac{3}{\pi\rho a\sigma_A{}^2}}\right)^3 \quad (4.8)$$

Thus, at fixed small Δy, the effective χ-parameter is predicted to increase strongly as the fraction of the random copolymer corresponding to the *more flexible* (smaller σ) species *increases*. Such a trend has been observed in PE/PEE random copolymer binary mixtures.[4,6] The dependence of the predicted deviations from mean-field theory *on temperature* is a subtle effect which enters via the T-dependent change in density and the species aspect ratios. Enhancement, reduction, or near insensitivity of the non-mean-field effects upon change of temperature are all possible depending on system-specific factors.

Table 3. Reduced χ-parameter, $10^4\chi_H/[\beta U_A^{(0)}(\Delta y)^2]$, at $\bar{y}$ = 0.5 for the Random Copolymer Composition Blends Shown in Figure 3a–c

	λ			
A/B	0.8	1.0	1.12	1.2
PEE/PE	15.2	71.4	252	433
PP/PE	57.3	21.8	144	288
PE/PTFE	206	4.7	26.7	101

All the general conclusions discussed above are in qualitative agreement with the prior analytic PRISM analysis of Schweizer[18] for the *thread blend problem based on the new molecular closure scheme*[15,16] *and the compressibility route to the thermodynamics*. This agreement is encouraging with regards to the robustness of our predictions to different thermodynamic routes and technical approximations within the liquid-state integral equation approach.

Model calculations based on eqs 4.5 and 4.6 for the thread PRISM χ-parameter as a function of the average copolymer composition are shown in Figure 3. Equation 4.6 in its aspect ratio version is employed

$$\Gamma^2(y) \cong y\Gamma_A{}^2 + (1-y)\Gamma_B{}^2 \quad (4.9)$$

with values of the aspect ratios appropriate for several experimentally interesting systems at 430 K (see Table 1). The selected aspect ratios correspond to polyethylene and poly(ethylethylene), i.e., EB(y) random copolymers (Figure 3a), polyethylene and polypropylene, i.e., EP(y) random copolymers (Figure 3b), and polyethylene and poly(tetrafluoroethylene) (Teflon) random copolymers (Figure 3c). Results are shown for several values of the *elementary* chemical asymmetry parameter, λ, which describes the chemical interaction differences between the A and B monomers. The plots are normalized to emphasize the shape and amplitude of the deviations from Flory theory (a horizontal line). Predicted magnitudes of χ scaled in the mean-field manner are listed in Table 3 for $\bar{y} = 0.5$.

For the EB(y) and EP(y) polyolefin alloys the chemically symmetric case of $\lambda = 1$ is a reasonable approximation. Alternatively, *a priori* estimates of λ based on group contribution methods[46] and the *assumption* that such procedures indicate solely the bare chemical effects (i.e., not local packing differences due to chain stiffness variations), yield $\lambda = 1.06$ and 1.077 for EB and EP alloys, respectively. That is, polyethylene has a larger *bare* solubility parameter than the vinyl polymers due to polarizability density differences between methylene, methyl, and methyne groups. For the polyethylene/Teflon system a crude estimate yields $\lambda \cong 0.8$; i.e., Teflon is the conformationally stiffer polymer but has weaker interchain dispersion interactions on a per unit volume basis.

There are several noteworthy trends displayed by Figure 3a–c.

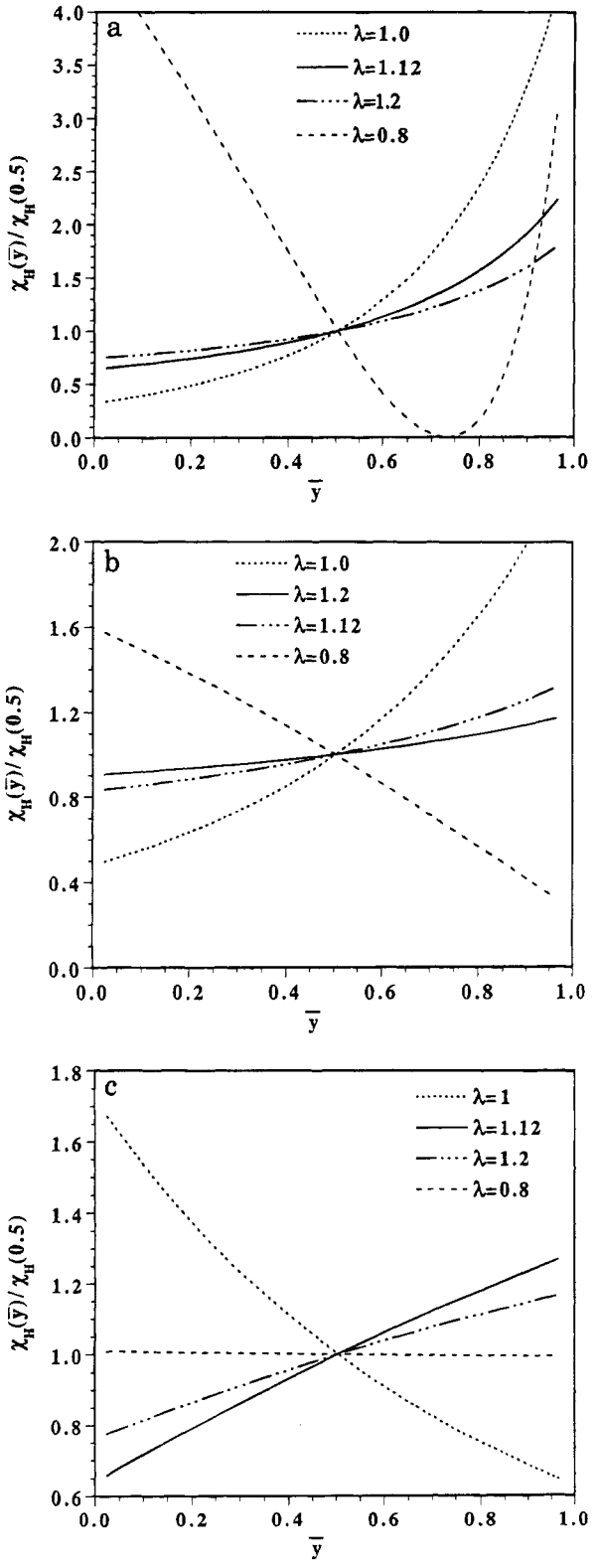

Figure 3. Normalized (at $\bar{y} = 0.5$) plot of the predicted χ-parameter of the binary random copolymer composition blend as a function of the average fraction of A-species for several values of chemical asymmetry λ. The compositional difference variable is fixed at $\Delta y = 0.1$. Three cases are considered corresponding to the choice of aspect ratios. (a) $(\Gamma_A,\Gamma_B) = (0.76,1.21)$ corresponding to PEE and PE. (b) $(\Gamma_A,\Gamma_B) = (0.93,1.21)$ corresponding to PP and PE. (c) $(\Gamma_A,\Gamma_B) = (1.41,1.21)$ corresponding to Teflon and PE.

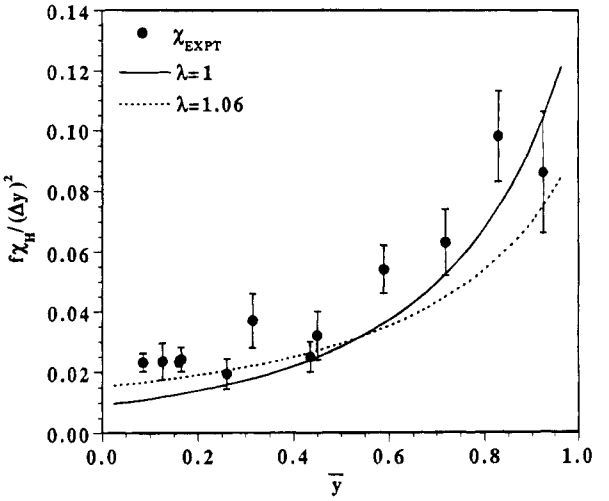

Figure 4. Predictions for the χ-parameter (on a four carbon basis) scaled in the mean-field manner as a function of the average composition variable for parameters representative of the PE/PEE random copolymer at 440 K. Experimental SANS data of Graessley et al.[4] are also shown, with estimated errors bars indicated. The theoretical results have been multiplied by the (of order unity) factor f as described in the text.

(1) We find (not shown) that the dependence of $\chi_H/(\Delta y)^2$ on Δy is very weak, essentially unresolvable on the scale of Figure 3 for a wide range of Δy values of 0.05–0.5. For this reason all our results are shown for a fixed value of $\Delta y = 0.1$.

(2) For the chemically symmetric $\lambda = 1$ case, the χ-parameter does depend strongly on mean copolymer composition and is predicted to always *increase as the mean aspect ratio of the blend decreases*. The magnitude of the predicted effect in Figure 3a is comparable to, although a little larger than, the recent polyolefin experimental observations on PE/PEE random copolymer blends.[4,6] If there is a bare chemical interaction asymmetry $\lambda > 1$, as is present to some degree in real polyolefin alloys, then the deviation from Flory–Huggins behavior is *reduced*.

(3) For the chemically symmetric $\lambda = 1$ case the dependence of χ on $\bar{y}$ decreases as the difference in the aspect ratio decreases and/or as the mean aspect ratio of the A and B homopolymers increases.

(4) At fixed aspect ratio asymmetry, the deviations from mean-field theory are quite sensitive to the chemical asymmetry parameter. There are distinct differences between the case where the stiffer chain is the stronger interacter versus when the stiffer chain is the weaker interacter. This again reflects the fundamental nonadditivity of the consequences of chemical and conformational asymmetries, and the possibilities of asymmetry compensation or reinforcement.[18]

(5) When the structural and chemical interaction asymmetries tend to compensate, it is possible for a nonmonotonic dependence of the χ-parameter on mean composition to occur.[18] This results in "windows of miscibility" as commonly observed in random copolymer systems[45,47] of practical importance (see Figure 3a).

(6) As predicted based on eq 4.7, if the chemical asymmetry is much larger than the conformational mismatch, then mean-field behavior (or nearly so) is recovered (see Figure 3c).

(7) The magnitudes of the predicted χ-parameters for $\bar{y} = 0.5$ are listed in Table 3. Again, strong nonadditivity and nonmonotonic dependence on the conformational and structural asymmetries is found.

Detailed applications to experimental polyolefin and polydiene systems will be presented in our companion paper.[10] As an example we show in Figure 4 results

for the χ-parameter on a four carbon basis for binary blends of EB(y) random copolymers at $T = 440$ K. The experimental SANS results are taken from Table 3 of ref 4. For the two sensible values of the PE/PEE chemical interaction asymmetry variable discussed above, good agreement between the theoretical predictions and the SANS data is obtained *without any fitting*. The only thing that has been adjusted to make the comparison is the overall scale of the theoretical χ-parameter via the factor f which equals $1/2\beta U_A^{(0)}$ for the $\lambda = 1.06$ case and $1/\beta U_A^{(0)}$ for the $\lambda = 1$ case. From eq A2 the factor f is roughly 0.2 and 0.37, respectively. This implies our *a priori* calculations of χ are roughly a factor of 2.5−5 too big, which is the same level of accuracy found for other polyolefin blends as discussed in section III.C.

We note that it is trivial to treat other random copolymer binary alloy cases, e.g., AB random copolymer plus C homopolymer, AB random copolymer plus CD random copolymer blend, etc. A solubility parameter is assigned to each polymer species according to eq 4.4 and an effective stiffness according to eq 4.6 or 4.9, and the net χ-parameter is simply given by eq 3.15. For example, the AB/C random copolymer/homopolymer blend is characterized by two distinct chemical interaction asymmetry parameters and three elementary statistical segments lengths determined by the structure of the A, B, and C monomers. A classic "random copolymer solubilization" phenomenon is predicted. That is, even if blends of A and B, A and C, and B and C are all strongly incompatible, if the solubility parameter of the C component is in between that of A and B, then small χ-parameters, and hence miscibility windows, are possible for certain ranges of AB composition.[45]

Finally, we note that enthalpy-based Flory-like approaches to random copolymer alloys have been developed and successfully applied to interpret miscibility in some systems.[45,48] However, these approaches are characterized by a plethora of empirical χ-parameters for the various pair (and often triad and possibly higher order) interactions. This contrasts strongly with our present microscopic approach which does not introduce multiple phenomenological χ-parameters and carries out the "averaging" of intra- and intermolecular interactions at the level of the Hamiltonian and hence solubility parameter. "Interference" effects and cancellation of destabilizing repulsive interactions occur at the level of the solubility parameter. If the fundamental chemical interaction and conformational parameters are known or can be estimated, then the theory can be applied in an *ab initio* manner to look for windows of miscibility and construct "miscibility maps" of random copolymer alloys in the same spirit as the phenomenological Flory-like approaches.[47]

V. Deuteration Swap Effect

A special case of the asymmetry competition effect discussed in section III.C is the deuteration swap experiment extensively studied recently by Crist et al.[42] and Graessley et al.[5,43] via SANS and cloud-point measurements. Since deuteration is believed to decrease the bond polarizability by ≅1%,[49] the corresponding chemical asymmetry parameter λ will be increased or decreased by essentially the same factor depending on which component is labeled. The theory of section III predicts that such deuteration will raise χ if the labeled species has the smaller melt solubility parameter, but lower χ if the larger melt solubility parameter species is deuterated. Such behavior applies universally to binary mixtures, i.e., to homopolymer blends, random copolymer alloys, random copolymer/homopolymer blends, etc. This swap effect is fundamentally inconsistent with the idea that the conformational asymmetry and chemical asymmetry effects are purely additive.

In terms of the general result of eq 3.14, deuteration simply decreases the labeled species interaction energy by a factor f_D, which depends on the amount of deuteration (i.e., partial versus full). At the level of the solubility parameter, this factor for chain M is

$$f_{D,M} = 1 - \Omega_M x_{D,M} \tag{5.1}$$

where $x_{D,M}$ is the fraction of polymer M which is deuterated. Prior estimates[49] suggest $\Omega_M \cong 0.01-0.016$. As discussed in the appendix, if one requires that the thread PRISM theory exactly reproduces the measured value of the SANS χ by Londano et al. for isotopic polyethylene blends,[51] then we obtain $\Omega_M \cong 0.012$. *PVT*-based experimental measurements[8] of melt solubility parameters for low branch content ethylene/butene random copolymers find a solubility parameter ratio of ≅1.006, thereby implying $\Omega_M \cong 0.006$. For polystyrene blends, Dudowicz et al.[51] suggest even smaller values of $\Omega_M \cong 0.001$.

The swap effect can be quantified by the ratio of χ-parameters

$$R \equiv \chi(f_{D,A})/\chi(f_{D,B}) \tag{5.2}$$

Since the factor f_D is very close to unity, eq 5.2 can be written as

$$R \cong \left[\frac{1 - \Omega_A x_A \dfrac{\delta_{AV}}{\Delta\delta}}{1 + \Omega_B x_B \dfrac{\delta_{AV}}{\Delta\delta}}\right]^2 \tag{5.3a}$$

where the average and difference solubility parameters refer to the *un*deuterated species and are defined in eqs 2.9b and 2.11a. Alternatively, R can be expressed as

$$R \cong \left[\frac{1 - \Omega_A x_A \left(\dfrac{-\beta U_{AV}}{2\chi_H}\right)^{1/2}}{1 + \Omega_B x_B \left(\dfrac{-\beta U_{AV}}{2\chi_H}\right)^{1/2}}\right]^2 \tag{5.3b}$$

where U_{AV} and χ_H are the average cohesive energy and χ-parameter of the *un*deuterated blend. If the B-species has the larger solubility parameter, then $R > 1$. This corresponds to the prediction that deuteration of the larger (smaller) δ polymer stabilizes (destabilizes) the blend, in accord with experimental observations on ethylene/butene-1 random copolymer mixtures[5,42,43] and also blends of alternating poly(styrene/methyl methacrylate) with PMMA homopolymers.[50] As a general point, since the average cohesive energy density is of order the thermal energy, eq 5.3b explains why the deuteration swap effect can be large for blends with small χ-parameters.

The influence of temperature on the amplitude of the swap effect may be subtle since it depends on the T-dependence of the undeuterated χ-parameter and the average cohesive energy (which are nonuniversal). However, for many systems the temperature depen-

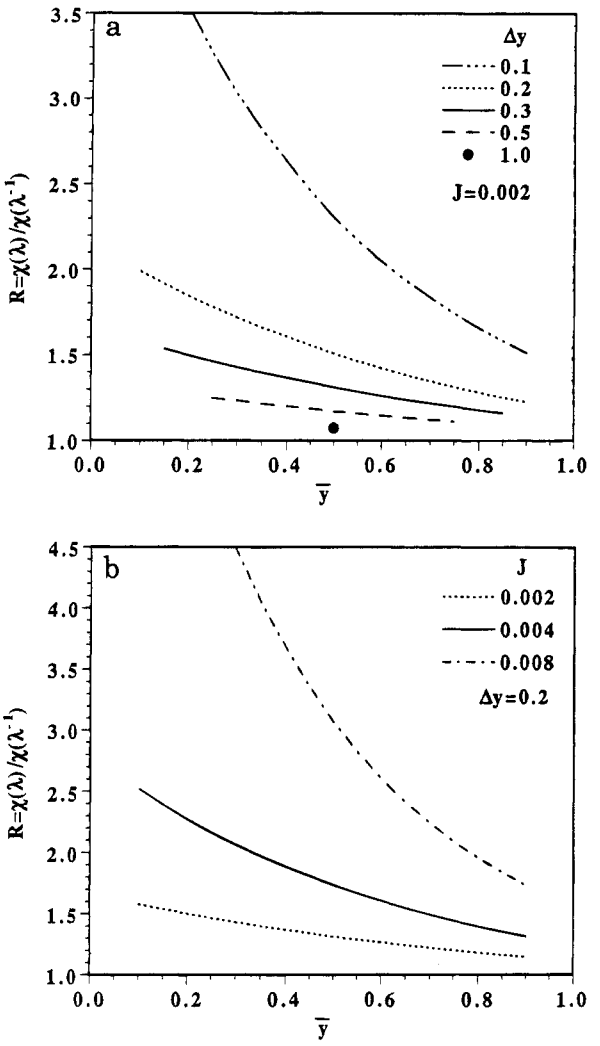

Figure 5. (a) Calculations of the swap effect χ-parameter ratio for a polymer model and parameters representative of PE/PEE random copolymers. Several values of the compositional difference variable are shown. The quantity J is the product of the percent deuteration and the magnitude of the energetic deuteration effect, i.e., $J = x_D\Omega$ in eq 5.1. (b) Same as Figure 5a but for fixed compositional difference and variable strength of the deuteration effect J.

dence of R may be rather weak since to leading order in T^{-1} it cancels out in eq 5.3b.

In many cases where the underlying solubility parameter differences are relatively large (e.g., PE + PEE homopolymer blends), R may be close to 1 and the swap effect is a small perturbation. However, for blends of random polyolefin copolymers of typical compositional differences (Δy = 0.1−0.3), the factor R is found experimentally[5,42,43] to be quite large (1.2−1.8) even for partial deuteration (roughly 35%). These observations are consistent with our analysis, and detailed applications to polyolefin experimental systems are presented in the companion paper.[10]

Model calculations are presented in Figure 5 for the idealized case of perfect "chemical interaction symmetry" at the (undeuterated) bare level, $\lambda = 1$. The calculations employ eqs 3.14 and 3.21, the same random copolymer model described in section IV, and the parameters used in Figure 3a which are typical of PE/PEE copolymers.[36] The factor f_D in eq 5.1 is taken to be identical for the A and B labeled chain cases. Again, our convention is such that $R > 1$ since the B-chain is defined to have the larger aspect ratio (and hence larger undeuterated melt solubility parameter). Results are shown in Figure 5a for a fixed value of f_D corresponding to a partial deuteration of roughly 33% (for $\Omega_M \cong 0.006$), as a function of the mean random copolymer composition and various composition difference values including the limiting case of a homopolymer blend of PE and PEE. The predicted magnitude of the swap effect is consistent with experiments on EB random copolymer blends.[5]

An example of the predicted effect of increasing the deuteration level for fixed composition difference is shown in Figure 5b. Note that the magnitude of the swap effect decreases as the structural asymmetry Δy increases, the mean aspect ratio decreases, and the level of deuteration decreases. These trends are a consequence of the diminishing importance of chemical interaction asymmetry relative to conformational asymmetry.

In experimental applications, the magnitude of the swap effect depends on the level of deuteration but may also depend on chain microstructure. This is because deuterons on the backbone of a branched polymer will not interact with intermolecular neighbors as well as deuterons on a side group due to the local correlation hole effect. Such behavior has been recently documented experimentally for polystyrene.[52] Thus, we expect the parameter Ω is a *maximum* for a purely main-chain polymer such as polyethylene. Hence, for random deuteration the effective value of Ω_M is expected to decrease with increasing PEE content for EB(y) alloys.

VI. Temperature Dependence of χ-Parameter

The temperature dependence of experimentally deduced effective χ-parameters is often (but not always) of the simple empirical form

$$\chi_{eff} \cong A + B/T \tag{6.1}$$

The factors A and B can be either positive or negative and are really just empirical fit parameters. However, they are often called the entropic and enthalpic contributions, respectively. Designating A as entropic would perhaps be appropriate if eq 6.1 really represented the leading correction to the infinite temperature limit. However, this is never the case. Experiments are performed over rather narrow temperature windows, generally never less than 250 K or more than 500 K. Thus, A and B represent apparent quantities in a restricted temperature window, and their entropic and enthalpic designations may be misleading with regards to the physical origin of these factors.

In this section we show that, within the very simple, purely enthalpic based χ-parameter of eq 3.14, a form such as eq 6.1 can emerge with A and B factors of *either sign* even for nonpolar hydrocarbon blends. The reason for this is simple to understand. The mean field T^{-1} dependence enters as a trivial prefactor in eq 3.14, but additional temperature dependencies arise from the solubility parameters in eq 3.15. For the thread model the density ϱ and effective segment length σ depend on temperature in a nonuniversal fashion. This results in a χ_H not simply proportional to inverse temperature (nor even necessarily monotonic) over a wide temperature interval. A wide spectrum of experimental behaviors is predicted to be possible depending on the detailed nature of these additional temperature dependences.

We begin the analysis by rewriting eq 3.14 in terms of a "reference temperature", T_0,

$$\chi_H = \frac{1}{2k_BT}(4\pi\varrho a^3\epsilon_{AA})\{\lambda\tilde{\delta}_B - \delta_A\}^2 \tag{6.2}$$

$$\tilde{\delta}_M = \frac{1}{\left(1 + c\frac{\varrho_0\sigma_0^2}{\varrho\sigma_M^2}\right)^{1/2}} \tag{6.3}$$

where c is a numerical constant. Equation 6.3 is expressed in terms of a reference melt system (subscripts "0"). As discussed in ref 36 and the appendix, if the reference state is chosen to be polyethylene at 430 K, then $c = 2 \times 0.176 = 0.352$. This is determined by the "calibration" requirement that the thread reduced solubility parameter be equal to its atomistic RIS analog.[36] For simplicity, and consistent with our constant volume assumption, we take the densities of the A and B melts to be equal at all temperatures(generalization is trivial).

We now estimate the T-dependence of χ in the neighborhood of the reference temperature by expanding the density and effective segment lengths through lowest order in $T - T_0$

$$\varrho \cong \varrho_0\left(1 + \left.\frac{d(\ln\varrho)}{dT}\right|_0 (T - T_0)\right) \equiv \varrho_0(1 + \alpha_\varrho\Delta T) \tag{6.4}$$

$$\sigma_M^2 \cong \sigma_{o,M}^2\left(1 + \left.\frac{d(\ln\sigma_{0,M}^2)}{dT}\right|_0 (T - T_0)\right) \equiv \sigma_{0,M}^2(1 + \delta C_M\Delta T) \tag{6.5}$$

where α_ϱ is the thermal expansion coefficient and δC_M is the logarithmic derivative of the characteristic ratio of polymer M in the melt, both evaluated at the reference temperature. Substituting these expressions into eqs 6.2 and 6.3, and collecting terms linear and independent in inverse temperature, yields a χ-parameter of the form of eq 6.1 where

$$A = k_B\chi_H(T_0)\, Q \tag{6.6}$$

$$B = k_BT_0\chi_H(T_0)\,\{1 - Q\} \tag{6.7}$$

$$Q \equiv T_0\left\{\alpha_\varrho + c\left(\frac{\sigma_0^2}{\sigma_{0,B}^2}\right) \times \frac{\lambda\tilde{\delta}_B^3(\alpha_\varrho + \delta C_B) - \tilde{\delta}_A^3\gamma^2(\alpha_\varrho + \delta C_A)}{\lambda\tilde{\delta}_B - \tilde{\delta}_A}\right\} \tag{6.8}$$

All blend quantities are evaluated at T_0. The ratio of the two factors is

$$\frac{A}{B} = -\frac{1}{T_0}(1 - Q^{-1})^{-1} \tag{6.9}$$

Depending on the sign and magnitude of Q relative to unity, *any sign* of A, B, or A/B can occur, and thus any type of temperature dependence of χ can occur. The various possibilities are schematically illustrated in Figure 6, which emphasizes that simple mean-field behavior occurs at (hypothetically) high temperatures

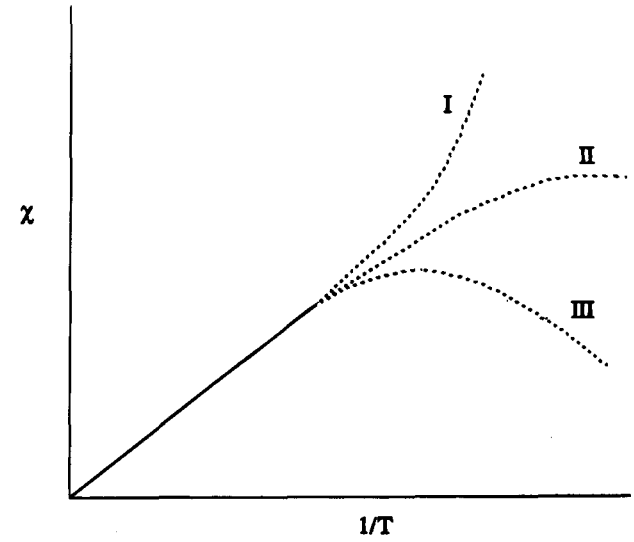

Figure 6. Schematic plot of three possible temperature dependences of the χ-parameter predicted by the PRISM solubility parameter theory. The low T part of the dotted lines are meant to indicate what might be measured in the experimental temperature window and fit by a straight line. In terms of the A and B parameters, the basic cases are $A < 0$ and $B > 0$ (case I), $A > 0$ and $B > 0$ (case II), and $A > 0$ and $B < 0$ (case III).

but nonuniversal deviation generally will occur in the experimentally accessible temperature window. Although the thermal expansion coefficient makes a negative contribution to Q in eq 6.8, the second complicated term can be of highly variable magnitude and *either sign* depending in a subtle way on the magnitudes of the conformational and chemical interaction asymmetries, and the chain expansion coefficients of each of the species. In particular, note that if $Q > 1$, then $A > 0$, $B < 0$, and the χ-parameter decreases upon cooling (case III in Figure 6). Such behavior is often associated with "specific AB interactions" and negative low-temperature χ-parameters but can apparently occur for chemically simple blends for different reasons (but still of local enthalpic origin). Such behavior is indeed predicted by the theory[10] (and observed) for certain polydiene blends (e.g., 1,4-polyisoprene and 1,2-polybutadiene (PVE)[44]). On the other hand, binary mixtures of random ethylene–butene-1 copolymers show more "normal" behavior corresponding to $A < 0$, $B > 0$, and A/B in the range of -0.001 to -0.002,[10] as observed experimentally.[4-8]

A special case of interest is *isotopic* mixtures.[53] For this structurally symmetric case the factor Q greatly simplifies

$$Q \equiv T_0\left\{\alpha_\varrho + c\frac{\sigma_0^2}{\sigma^2}\tilde{\delta}^2(\alpha_\varrho + \delta C)\right\} \tag{6.10}$$

where the unlabeled quantities at the reference temperature are now species independent. It is interesting to note that the chemical (isotopic) asymmetry parameter λ has *cancelled out*. Thus, eqs 6.7 and 6.6 predict that A and B are *both* proportional to the fraction of deuteration squared since they have a common origin, dispersive interactions. Such behavior has been seen in SANS experiments on isotopic mixtures of poly(ethylenepropylene) (PEP),[54] which provides support for our contention that it is often misleading to think of A as an entropic contribution. For most isotopic blends we find that $A < 0$, $B > 0$, and A/B is of order -0.001.

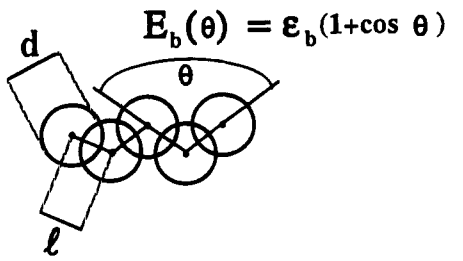

Figure 7. Schematic illustration of the discrete, overlapping site semiflexible chain (SFC) model.

As discussed elsewhere,[10] this prediction agrees with many (but not all) experimental SANS studies on isotopic mixtures. The complex T-dependences of χ sketched in Figure 6 will have strong consequences for the apparent N-dependence of critical and spinodal temperatures.

Finally, we emphasize two important caveats. First, all systems are not expected to obey eq 6.1, and more complicated behavior is possible based simply on eq 3.14 (e.g., nonmonotonic dependence of χ on T). Second, we are not claiming that for all systems the quantities A and B are of purely enthalpic origin, and explicit entropic contributions are unimportant. However, applications of the above formulas to predict the temperature dependences of experimental isotopic, polyolefin, and polydiene blends suggest that the purely enthalpic interpretation has widespread relevance.[10]

VII. Numerical Predictions for Semiflexible Chains

In this section we employ the overlapping semiflexible chain (SFC) model plus melt PRISM theory[2,3] to numercially investigate the χ-parameter. The discrete SFC model,[55] and the relationship of its parameters to real polymer structures, has been discussed in depth elsewhere.[36] The model is shown schematically in Figure 7. The important feature is that there are three local length scales: (i) chain thickness or repeat unit diameter d, (ii) an effective site−site separation (bond length l) which controls the amount of surface area available for interchain packing, and (iii) a persistence or statistical segment length which is controlled by a local bending potential of the form $\epsilon_b(1 + \cos(\theta))$ which introduces local rigidity to the backbone. Based on geometric considerations and the desire to have the SFC model mimic the packing correlations of real polymers (e.g., realistic local correlation holes in $g(r)$), we have chosen a single value of $l/d = 0.5$.[36] The density of the fluid is describable in terms of the dimensionless quantity ϱd^3, which is taken to be the melt value of 1.375. This value is deduced according to a calibration procedure which ensures the compressibility of PE at 430 K is reproduced by the coarse-grained SFC model.[36]

Since the SFC model does not contain side groups, the effect of branching and tacticity enters only indirectly via an effective backbone stiffness. One must keep in mind that this scheme is a crude one which neglects physical features such as side-group interdigitation and/or specific packing arrangements. PRISM theory has been recently generalized to explicitly treat chain branching by Curro.[56]

Based on the estimates in Table 1, the flexible polymers of interest are characterized by aspect ratios of order unity, and all the various estimates for polyolefins, polydienes, polystyrenes, etc., fall in the small range of $\Gamma \cong 0.7-1.4$.[36] Since polymers display widely variable changes of their characteristic ratios with temperature, the relative values of the aspect ratios can vary in a subtle manner with T.

Table 4. SFC Model ($l/d = 0.5$, $N = 2000$) Calculations of the Thermal χ-Parameter Based on equations 2.6 and 7.1 for the Chemical Interaction Symmetric Case ($\lambda = 1$) and a Melt Reduced Density of 1.375[a]

Γ_A	Γ_B	$10^3\chi_H/\beta\epsilon$	$\Gamma_B^4\chi_H/\beta\epsilon(\gamma^2-1)^2$	$10^3\chi^{(0)}$
0.8	0.85	8.6	0.27	−0.01
0.8	0.9	35.2	0.33	−0.03
0.8	1.0	143.9	0.45	−0.08
0.8	1.2	398.8	0.53	0.14
0.8	1.4	566.2	0.51	0.79
0.85	0.9	9.0	0.40	−0.01
0.85	0.95	35.0	0.40	−0.02
0.85	1.05	125.3	0.55	−0.02
0.9	0.95	8.5	0.53	0.00
0.9	1.0	36.8	0.67	0.00
0.9	1.1	108.1	0.65	0.06
0.95	1.0	9.9	0.85	0.00
0.95	1.05	27.9	0.69	0.02
0.95	1.15	87.4	0.71	0.15
1.0	1.025	0.83	0.36	0.00
1.0	1.05	4.6	0.53	0.01
1.0	1.1	18.7	0.62	0.04
1.0	1.2	63.6	0.53	0.21
1.0	1.4	139.2	0.58	0.76
1.025	1.05	1.5	0.75	0.00
1.05	1.1	4.8	0.74	0.01
1.05	1.15	16.6	0.73	0.06
1.05	1.25	48.2	0.68	0.25
1.1	1.2	13.3	0.76	0.08
1.1	1.3	34.0	0.62	0.27
1.2	1.4	14.6	0.43	0.25
1.3	1.4	2.69	0.40	0.07
1.35	1.4	0.55	0.37	0.02

[a] The purely athermal χ-parameter, $\chi^{(0)}$ (multiplied by 1000), for a $\phi = 0.5$ blend computed using eq 7.2 is also shown (to two significant digits).

A. Thermal χ-Parameter. We have carried out a systematic numerical study of the predicted *constant volume* Hildebrand χ-parameter of eq 2.6 using the SFC model, for many pairs of aspect ratios ($\Gamma_A < \Gamma_B$) and many values of the chemical asymmetry variable λ. The attractive potential employed is of a Lennard-Jones-like form

$$v_M(r) = \epsilon_M\left[\left(\frac{d}{r}\right)^{12} - 2\left(\frac{d}{r}\right)^{6}\right], \quad r \geq d \qquad (7.1)$$

A representative set of our numerical results is listed in Table 4 for the "interaction symmetric" $\lambda = 1$ case (bare Flory $\chi = 0$, i.e., $\epsilon_{MM'} = \epsilon$). Our predicted enthalpic χ-parameter both divided by $\beta\epsilon$, and scaled in a manner predicted by the thread analysis of eq 3.18, is shown.

The basic trends in Table 4 are easy to understand from examining the calculated reduced melt solubility parameter (see Figure 8a), and the square of the reduced solubility parameter difference (see Figure 8b), as functions of chain aspect ratio.[36] Since δ increases monotonically with the aspect ratio, the predicted χ-parameter increases monotonically with the aspect ratio difference $\Delta\Gamma = \Gamma_B - \Gamma_A$. However, for a fixed $\Delta\Gamma$, the χ-parameter decreases significantly as the mean aspect ratio $2\Gamma = \Gamma_B + \Gamma_A$ increases since the melt solubility parameter tends to increase more slowly at high aspect ratios. Note also that since for experimental hydrocarbon systems $\beta\epsilon \cong 1$ on a four carbon basis for our model,[36] the enthalpic χ-parameters are generally large by polymer standards, even for the interaction symmetric case considered here.

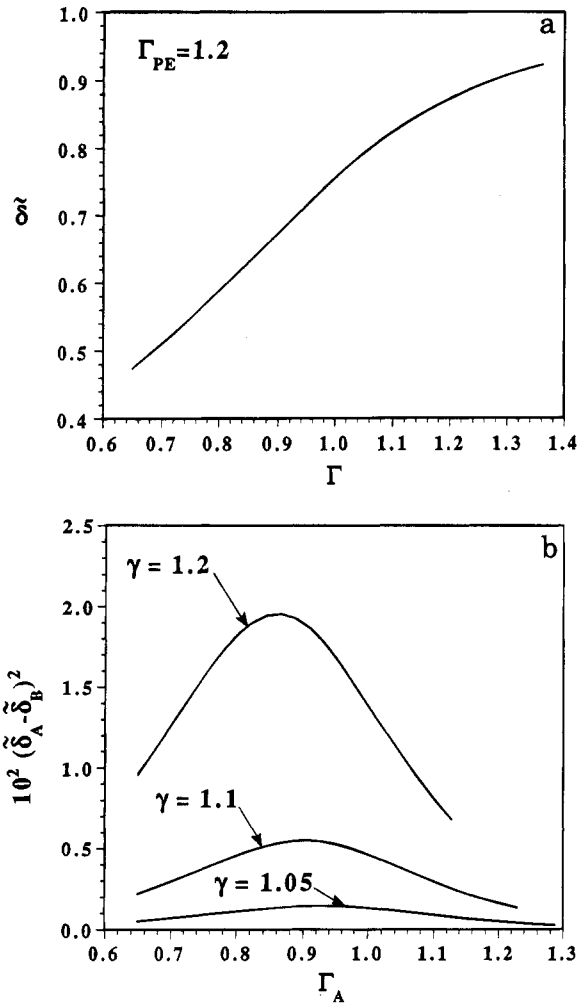

Figure 8. (a) Reduced solubility parameter of SFC melts as a function of the chain aspect ratio. This curve has been "calibrated" assuming a polyethylene aspect ratio of 1.2 at 430 K (see ref 36). (b) Square of the difference of SFC reduced solubility parameters as a function of the A-chain aspect ratio for a melt reduced density and several values of the conformational asymmetry parameter $\gamma = \Gamma_B/\Gamma_A$.

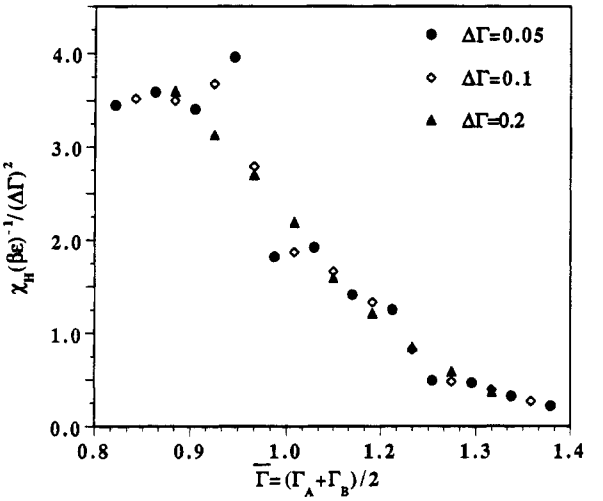

Figure 9. Scaled χ-parameter for the SFC homopolymer melt model as a function of the mean aspect ratio for three values of aspect ratio difference $\Delta\Gamma = \Gamma_B - \Gamma_A$ (shown as different shape symbols) and many distinct choices of (Γ_B, Γ_A). All results are for the chemically symmetric case corresponding to $\lambda = 1$.

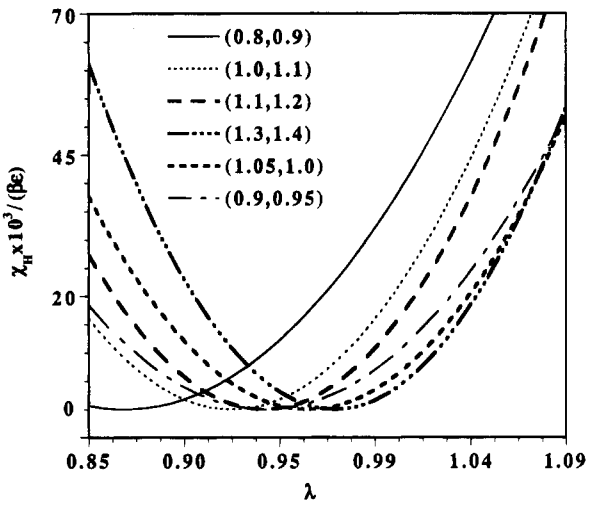

Figure 10. Scaled χ-parameter versus chemical asymmetry variable for several indicated choices of chain aspect ratios (Γ_A, Γ_B).

The absolute magnitudes and general trends of the predicted χ-parameters in Table 4 are quite similar to the thread-based values, although quantitative differences certainly exist as expected. The thread-based scaling of eq 3.18 is not perfect, but it does a remarkable job of organizing the SFC predictions. For example, although the SFC χ-parameter varies by roughly *3 orders of magnitude* depending on the aspect ratio pair considered, the scaled χ-parameter varies only by roughly a factor of 2.5. This demonstrates both a significant robustness of our predictions to local modifications of the single-chain model and the apparent usefulness of the effective aspect ratio idea.

As discussed in depth elsewhere,[36] the precise *quantitative* values of aspect ratios appropriate for a real polymer modeled as a SFC are different than for the Gaussian thread, although relative values are qualitatively unchanged. The question of which of the coarse-grained models, thread or SFC, is "more appropriate" for real experimental alloys is a subtle one which is not possible to definitively answer at present.

In Figure 9 an attempt to generate a "master" curve for the $\lambda = 1$ case is presented. For many values of (Γ_A, Γ_B) and several distinct $\Delta\Gamma$ values, a χ-parameter scaled in the spirit of the random copolymer problem is plotted versus mean aspect ratio. Perfect collapse does not occur, but an approximate collapse onto a single curve is obtained which has an interesting shape. The roughly monotonic decrease of the scaled χ-parameter above a mean aspect ratio of $\cong$0.85 implies the deviations from mean-field random copolymer theory are qualitatively the same for the thread and SFC models.

In Figure 10 we present representative results for the effect of chemical interaction asymmetry. As in the thread model, a nonmonotonic behavior is found with χ going to zero at a "perfect asymmetry compensation" point. Such a perfect asymmetry compensation is not expected to occur in reality due to corrections to the solubility parameter approach (e.g., mixing volume changes). Whether the introduction of chemical asymmetry stabilizes or destabilizes the blend depends on the precise values of the chemical asymmetry parameter and the aspect ratios.[18]

B. Athermal χ-Parameter and Nonlocal Entropic Effects. We have also computed the purely *athermal* χ-parameter for the conformationally asymmetric *binary blend*. The numerical blend PRISM

procedure has been thoroughly discussed previously.[3,12-16] Results for an equal degree of polymerization 50/50 mixture are listed in Table 4. The calculations employ the compressibility route and utilize the Kirkwood–Buff relations for the Gibbs free energy. For an equal degree of polymerization and $\phi = 0.5$ the blend χ is given by:[14]

$$\chi^{(0)} \equiv \frac{2}{N} - \frac{1}{2}\frac{\partial^2 \beta\tilde{F}}{\partial\phi^2}$$

$$\frac{\partial^2 \beta\tilde{F}}{\partial\phi^2} = \varrho[\hat{S}_{AA}^{-1}(0)\,\hat{S}_{BB}^{-1}(0) - (\hat{S}_{AB}^{-1}(0))^2] \times \left[\frac{1}{\hat{S}_{AB}^{-1}(0) + \hat{S}_{BB}^{-1}(0)} + \frac{1}{\hat{S}_{AA}^{-1}(0) + \hat{S}_{AB}^{-1}(0)}\right] \quad (7.2)$$

where the matrix elements of the inverse partial structure factor matrix are given in terms of the $k = 0$ direct correlation functions as

$$\hat{S}_{MM'}^{-1}(0) = 2\frac{\delta_{MM'}}{N\varrho} - \hat{C}_{MM'}(0) \quad (7.3)$$

Note that the above χ-parameter is invariant to A/B interchange. In the noninteracting limit (defined as $\hat{C}_{MM'}(0) \to 0$), $\chi^{(0)} = 0$ as it must. Using eq 7.3 in eq 7.2 yields $\chi^{(0)}$ directly in terms of the $k = 0$ direct correlations as

$$\chi^{(0)} = \frac{2}{N} - \frac{\Xi}{2}\left[\varrho^2\{C_{AA}C_{BB} - C_{AB}^2\} + \frac{4}{N^2} - \frac{2}{N}\varrho(C_{AA} + C_{BB})\right]$$

where

$$\Xi \equiv \left[\frac{1}{-\varrho(C_{AB} + C_{BB}) + 2\varrho N^{-1}} + \frac{1}{-\varrho(C_{AB} + C_{AA}) + 2\varrho N^{-1}}\right] \quad (7.4)$$

and a shorthand notation has been used for the direct correlations functions at $k = 0$. Note that $\chi^{(0)}$ is not a linear function of the direct correlation functions as is obtained if a literal incompressibility constraint is employed.[3,12-18] The fundamental nonlinearity and presence of crossterms between the species-dependent direct correlation functions are very important features as emphasized previously.[17,18]

C. Summary and Interpretation. There are three important points concerning the results in Table 4.

(1) The sign of the athermal χ-parameter can be positive or negative depending primarily on the mean aspect ratio of the blend.

(2) For the cases presented in Table 4, the absolute magnitude of the *athermal* χ is relatively small; i.e., the product $\chi^{(0)}N$ is generally not close to the critical value of 2. However, as the mean aspect ratio of the blend increases, $\chi^{(0)}N$ can get close to the critical value. Athermal phase separation driven by "nonlocal excess entropic" effects is found for blends composed of long chains of higher aspect ratios, but the required values of the latter are not representative of flexible polymers.[34]

(3) For experimentally relevant temperatures $\beta\epsilon$ is a number of order unity. *Hence, for the cases in Table 4 the thermal, or enthalpic, χ-parameter associated with conformational asymmetry is predicted to be larger by roughly 2 to 3 orders of magnitude than its athermal counterpart.* This is our most important prediction and has profound experimental implications. If an experiment can be performed on the miscible blend, then since $\beta\epsilon$ is a number of order unity the athermal χ-parameter contribution is predicted to be swamped by the thermal contribution. This finding supports the solubility parameter or Hildebrand assumption that local enthalpic interactions are dominant. However, the athermal term may still play an important role in the sense of ruling out miscibility; i.e., if it is big, then mixing is impossible for purely packing reasons (excess entropy). Of course, by definition such cases are irrelevant to measurements in the one-phase region.

All our above conclusions for the athermal blend are based on the SFC model and the compressibility route to the thermodynamics. PRISM studies based on the so-called free energy or charging route are much more difficult to numerically perform, but we have recently investigated this approach.[34] The results are consistent in a semiquantitative sense with the compressibility route computations. The influence of microscopic, chemically-realistic structure and explicit chain branches on the excess entropy issue has begun to be investigated by Curro and Rajasekharan.[41]

Quantitative predictions using the SFC model and Hildebrand PRISM theory for the magnitude and temperature dependence of the χ-parameter, the deuteration swap effect, and the random copolymer blend problem will be presented elsewhere in the context of polyolefin applications.[11] Comparisons with full numerical blend calculations beyond the solubility parameter description have also been made.[11]

VIII. Discussion

In this paper we have formulated a microscopic theory of the thermodynamics of polymer blends at the level of solubility parameters using the homopolymer melt PRISM theory as input. We believe this is the simplest conceivable approach to constructing a microscopic theory of polymer alloy phase behavior which includes system-specific local correlation effects. More sophisticated, tractable free-energy-based approaches have also been outlined and will be studied in the future.

On the basis of both the analytically tractable thread model and the less coarse-grained semiflexible chain model, we have obtained predictions for the influence on blend compatibility of conformational and chemical interaction asymmetries, chain lengths, polymer density, attractive potential range, and (crudely) mixing volume changes. The purely enthalpic χ-parameter is influenced in a generally nonadditive manner by all these aspects due to their modification of local packing in the melt. In essence, these are melt "equation-of-state" effects known to be important in compressible fluids. Numerical estimates of χ for polyolefins yield numbers consistent with experimental magnitudes. A host of "non-Flory–Huggins" effects are predicted including (a) the failure of mean-field theory for random copolymer blends, (b) deuteration swap effects, (c) nonadditivity of chemical and structural asymmetry contributions to χ and the possibility of asymmetry "compensation", (d) possible significant contributions of volume changes to miscibility, and (e) possible unusual and subtle temperature dependences of χ due to thermally-induced density and chain dimension changes. Points d and/or e can even result in lower critical solution temperature (LCST) behavior in nonpolar

polymer alloys, as apparently observed in polydiene blends[44] and hinted at in certain polyolefin alloys[4-8] and the polystyrene/poly(*n*-butyl methacrylate) system.[57]

In our companion paper the simple PRISM solubility parameter theory is applied to a wide range of isotopic, polyolefin, and polydiene blends.[10] Comparison of the theoretical predictions with SANS and cloud-point experiments is encouraging. Nevertheless, as discussed in section II, there are certainly questions and effects which cannot be addressed within any melt solubility parameter approach. For example, the simple Hildebrand approach is incapable of properly addressing the question of a blend composition dependence of the χ-parameter, specific attractive interactions, and the possibility of a negative χ-parameter under constant volume conditions. Even accepting these limitations, there remain fundamental questions about the adequacy of the statistical mechanical approximations (1)–(4) invoked to derive the Hildebrand-like theory. Are the multiple approximations individually adequate, or might the errors conspire to cancel in many cases? These issues will be studied in forthcoming publications, as will the subtle questions of the adequacy of coarse-grained models versus fully atomistic descriptions such as the rotational isomeric state (RIS) model, and the relation of the free-energy perturbation PRISM approach to the compressibility route formulation based on the new molecular closures.

Acknowledgment. We are indebted to W. W. Graessley and R. Krishnamoorti for the stimulating discussions and preprints which motivated this work. We also thank R. Krishnamoorti for sending unpublished data from his thesis. E. F. David is acknowledged for many helpful discussions, a critical reading of the manuscript, and providing Figures 7 and 8. Helpful discussions with J. G. Curro, J. D. Londano, and G. D. Wignall are also appreciated. Funding was provided by the Division of Materials Sciences, Office of Basic Energy Sciences, U.S. Department of Energy in cooperation with Oak Ridge National Laboratory, and the UIUC Materials Research Laboratory (via Grant No. DEFG02-91ER45439).

Appendix: Coarse-Grained Model Parameters

The connection between the thread model parameters and those of real hydrocarbon molecules has been discussed in depth elsewhere.[36] This correspondence, or "mapping", between the thread and atomistic level descriptions can be employed to estimate the magnitude of the χ-parameter. There are four basic quantities: a = spatial range of attractive tail potential, ϱ = segmental number density, ϵ = energy parameter (well depth) of attractive tail potential, and σ = statistical segment length. The density enters the thread model in the reduced forms, ϱa^3 or $\varrho\sigma^2 a$. The parameters are determined by a "calibration procedure" as follows.

(1) The mean-field attractive energy per site (or cohesive energy) in the thread and RIS model of a polyethylene melt are equated. For the thread

$$U_M^{(0)} \equiv \varrho \int d\vec{r}\, v_M(r) = -4\pi\epsilon_M \varrho a_M^3 \qquad \text{(A1)}$$

For polyethylene, based on the Barker–Henderson division of the Lennard-Jones potential and standard parameters, the corresponding energy per methylene group is[36]

$$-U_{CH_2}^{(0)} \equiv \frac{32\pi}{9}\varrho_{CH_2}\epsilon_{CH_2}\sigma_{CH_2}^3 \cong 1200\ \text{K} \qquad \text{(A2)}$$

(2) The appropriate choice of a in eq 3.10 which reproduces the atomistic RIS level PRISM prediction for the reduced solubility parameter of a polyethylene melt at 430 K, $\tilde{\delta} = 0.86$, requires[36]

$$\tilde{\delta} = \frac{1}{(1 + [0.176/\varrho\sigma^2])^{1/2}} \qquad \text{(A3)}$$

where the invariant quantity $\varrho\sigma^2$ is expressed in inverse angstroms and equals 0.5 for polyethylene at 430 K. This calibration procedure is carried out for one polymer (polyethylene) at one temperature. Predictions for other polymers and temperatures are then made *a priori*.

(3) Values of the statistical segment length and effective aspect ratio are computed *a priori* using experimental chain parameters and density information based on the following relations:[36]

$$\sigma_{ref} \equiv \left(\frac{6R_g^2}{N_{mon}}\frac{V_{ref}}{V_{mon}}\right)^{1/2}, \qquad d_{ref} \equiv \left(\frac{6V_{ref}}{\pi}\right)^{1/3}$$

$$\Gamma_{ref} \equiv \sigma_{ref}/d_{ref} \qquad \text{(A4)}$$

where N_{mon} is the number of monomers (repeat units) and V_{mon} is the monomer volume estimated as the inverse of the monomer number density. Such a relation for the statistical segment length has been previously employed by Bates et al.[40] and Graessley et al.[8] Equation A3 can be rewritten in terms of this aspect ratio as

$$\tilde{\delta} = \frac{1}{(1 + 0.515/\Gamma^2)^{1/2}} \qquad \text{(A5)}$$

The bare "chemical" part of the solubility parameter, and hence the asymmetry variable λ, might be estimated from standard solubility parameter schemes based on a group additivity approximation.[46]

For the deuteration issues the parameter Ω which quantifies the chemical asymmetry for the fully deuterated isotopic blend is estimated as follows. It is required that the χ-parameter for the isotopic blend predicted by thread PRISM (see eq 4.2) exactly equals the experimental value measured by Londano and coworkers for polyethylene at 430 K: $\chi = 0.0002$ on a single carbon basis.[51] This constraint, coupled with the above analysis, yields $\Omega = 0.012$, which is consistent with prior estimates.[49]

References and Notes

(1) For a recent review, see: Binder, K. *Adv. Polym. Sci.* **1994**, *112*, 181.
(2) Schweizer, K. S.; Curro, J. G. *Phys. Rev. Lett.* **1987**, *58*, 246. Curro, J. G.; Schweizer, K. S. *Macromolecules* **1987**, *20*, 1928; *J. Chem. Phys.* **1987**, *87*, 1842. Schweizer, K. S.; Curro, J. G. *Macromolecules* **1988**, *21*, 3070, 3082.
(3) For a recent review of PRISM theory, see: Schweizer, K. S.; Curro, J. G. *Adv. Polym. Sci.* **1994**, *116*, 319.
(4) Graessley, W. W.; Krishnamoorti, R.; Balsara, N. P.; Butera, R. J.; Fetters, L. J.; Lohse, D. J.; Schulz, D. N.; Sissano, J. A. *Macromolecules* **1994**, *27*, 3896.
(5) Graessley, W. W.; Krishnamoorti, R.; Balsara, N. P.; Fetters, L. J.; Lohse, D. J.; Schulz, D. N.; Sissano, J. A. *Macromolecules* **1994**, *27*, 2574.
(6) Krishnamoorti, R.; Graessley, W. W.; Balsara, N. P.; Lohse, D. J. *Macromolecules* **1994**, *27*, 3073.

(7) Walsh, D. J.; Graessley, W. W.; Datta, S.; Lohse, D. J.; Fetters, L. J. *Macromolecules* **1992**, *25*, 5236.
(8) Graessley, W. W.; Krishnamoorti, R.; Reichart, G. C.; Balsara, N. P.; Fetters, L. J.; Lohse, D. J., preprint, 1994. Krishnamoorti, R. Ph.D. Thesis, Princeton University, Princeton, NJ, 1993.
(9) Rowlinson, J. S.; Swinton, F. L. *Liquids and Liquid Mixtures*; Butterworth Scientific: London, 1982. Hildebrand, J.; Scott, R. *The Solubility of Nonelectrolytes*; 3rd ed.; Reinhold: New York, 1949.
(10) Schweizer, K. S.; Singh, C. *Macromolecules*, to be submitted.
(11) Singh, C.; Schweizer, K. S., in preparation.
(12) Schweizer, K. S.; Curro, J. G. *J. Chem. Phys.* **1989**, *91*, 5059.
(13) Curro, J. G.; Schweizer, K. S. *Macromolecules* **1990**, *23*, 1402.
(14) Curro, J. G.; Schweizer, K. S. *Macromolecules* **1991**, *24*, 6736.
(15) Yethiraj, A.; Schweizer, K. S. *J. Chem. Phys.* **1992**, *97*, 5927; **1993**, *98*, 9080.
(16) Schweizer, K. S.; Yethiraj, A. *J. Chem. Phys.* **1993**, *98*, 9053.
(17) Schweizer, K. S. *Macromolecules* **1993**, *26*, 6033.
(18) Schweizer, K. S. *Macromolecules* **1993**, *26*, 6050.
(19) Singh, C.; Schweizer, K. S.; Yethiraj, A. *J. Chem. Phys.*, **1995**.
(20) Schweizer, K. S.; Curro, J. G. *Chem. Phys.* **1990**, *149*, 105.
(21) Curro, J. G.; Schweizer, K. S.; Grest, G.; Kremer, K. *J. Chem. Phys.* **1989**, *91*, 1357.
(22) Dodd, L. R.; Theodorou, D. N. *Adv. Polym. Sci.* **1994**, *116*, 249.
(23) Yethiraj, A.; Hall, C. K. *J. Chem. Phys.* **1991**, *93*, 4453; **1992**, *96*, 797.
(24) Honnell, K. G.; McCoy, J. D.; Curro, J. G.; Schweizer, K. S.; Narten, A. H.; Habenshuss, A. *J. Chem. Phys.* **1991**, *94*, 4659.
(25) Narten, A. H.; Habenshuss, A.; Honnell, K. G.; McCoy, J. D.; Curro, J. G.; Schweizer, K. S. *J. Chem. Soc., Faraday Trans.* **1992**, *13*, 1791.
(26) deGennes, P.-G. *Scaling Concepts in Polymer Physics*; Cornell University Press: Ithaca, NY, 1979.
(27) Schweizer, K. S.; Honnell, K. G.; Curro, J. G. *J. Chem. Phys.* **1992**, *96*, 3211. Yethiraj, A.; Schweizer, K. S. *J. Chem. Phys.* **1992**, *97*, 5927.
(28) Melenkevitz, J.; Schweizer, K. S.; Curro, J. G. *Macromolecules* **1993**, *26*, 6190. Melenkevitz, J.; Curro, J. G.; Schweizer, K. S. *J. Chem. Phys.* **1993**, *99*, 5571.
(29) Grayce, C. J.; Schweizer, K. S. *J. Chem. Phys.* **1994**, *100*, 6846. Grayce, C. J.; Yethiraj, A.; Schweizer, K. S. *J. Chem. Phys.* **1994**, *100*, 6857. Grayce, C. J.; dePablo, J. J. *J. Chem. Phys.* **1994**, *101*, 6014.
(30) Hansen, J. P.; McDonald, I. R. *Theory of Simple Liquids*, 2nd ed.; Academic Press: London, 1986.
(31) Andersen, H. C.; Chandler, D.; Weeks, J. D. *Adv. Chem. Phys.* **1976**, *34*, 105.
(32) Chandler, D. In *Studies in Statistical Mechanics VIII*; Montroll, E., Lebowitz, J., Eds.; North-Holland: Amsterdam, The Netherlands, 1982; p 274.
(33) Chandler, D. *Phys. Rev. E* **1993**, *48*, 2893.
(34) (a) Singh, C.; Schweizer, K. S. *J. Chem. Phys.*, submitted, 1995. (b) Weinhold, J.; Kumar, S.; Singh, C.; Schweizer, K. S. *Macromolecules*, submitted for publication.
(35) Bates, F. S.; Fredrickson, G. F. *Macromolecules* **1994**, *27*, 1065. Fredrickson, G. H.; Liu, A. J.; Bates, F. S. *Macromolecules* **1994**, *27*, 2503.
(36) Schweizer, K. S.; David, E. F.; Singh, C.; Curro, J. G.; Rajasekharan, J. J. *Macromolecules* **1995**, *28*, 1528.
(37) Doi, M.; Edwards, S. F. *The Theory of Polymer Dynamics*; Clarendon: Oxford, U.K., 1986. Muthukumar, M. *J. Chem. Phys.* **1986**, *85*, 4722.
(38) Ougizawa, T.; Dee, G. T.; Walsh, D. J. *Polymer* **1989**, *30*, 1675. See also, Orwell, R. A.; Flory, P. J. *J. Am. Chem. Soc.* **1967**, *89*, 6814.
(39) Chen, S.-J.; Chiew, Y. C.; Garddecki, J. A.; Nilsen, S.; Radosz, M. *J. Polym. Sci., Part B: Polym. Phys.* **1994**, *32*, 1791.
(40) Bates, F. S.; Schulz, M. F.; Rosedale, J. H. *Macromolecules* **1992**, *25*, 5547. Gehlsen, M. D.; Bates, F. S. *Macromolecules* **1994**, *27*, 3611.
(41) Rajasekaran, J. J.; Curro, J. G., in preparation.
(42) Rhee, J.; Crist, B. *Macromolecules* **1991**, *24*, 5663. Nicholson, J. C.; Finerman, T. M.; Crist, B. *Polymer* **1990**, *31*, 2287
(43) Balsara, N. P.; Fetters, L. J.; Hadjichristidis, N.; Lohse, D. J.; Han, C. C.; Graessley, W. W.; Krishnamoorti, R. *Macromolecules* **1992**, *25*, 6137.
(44) See, for example: Sakurai, S.; Jinnai, H.; Hasegawa, H.; Hashimoto, T.; Han, C. C. *Macromolecules* **1991**, *24*, 4839. Tomlin, D. W.; Roland, C. M. *Macromolecules* **1992**, *25*, 2994.
(45) Scott, R. L. *J. Polym. Sci.* **1952**, *9*, 423. ten Brinke, G.; Karacz, F. E.; MacKnight, W. J. *Macromolecules* **1983**, *16*, 1827. Kambour, R. P.; Bendler, J. T.; Bopp, R. C. *Macromolecules* **1983**, *16*, 753. Paul, D. R.; Barlow, J. *Polymer* **1984**, *25*, 487.
(46) Coleman, M. M.; Serman, C. J.; Bhagwagar, D. E.; Painter, P. *Polymer* **1990**, *31*, 1187. van Krevelin, *Properties of Polymers*; Elsevier: New York, 1972; p 55. Bicerano, J., Ed.; *Computational Modeling of Polymers*; Marcel Dekker: New York, 1992; Chapter 1.
(47) Zhikuan, C.; Ruona, S.; Karasz, F. E. *Macromolecules* **1992**, *25*, 6113 and references cited therein.
(48) Balacz, A. C.; Sanchez, I. C.; Epstein, I. R.; Karasz, F. E.; MacKnight, W. J. *Macromolecules* **1985**, *18*, 2188.
(49) Bates, F. S.; Fetters, L. J.; Wignall, G. D. *Macromolecules* **1988**, *21*, 1086.
(50) Galvin, M. E.; Heffner, S.; Winey, K. I. *Macromolecules* **1994**, *27*, 3520.
(51) Londano, J. D.; Narten, A. H.; Wignall, G. D.; Honnell, K. G.; Hseih, E. T.; Johnson, T. W.; Bates, F. S. *Macromolecules* **1994**, *27*, 2864. Dudowicz, J.; Freed, K. F.; Lifschitz, M. *Macromolecules* **1994**, *27*, 5387.
(52) Gomez-Elvira, J. M.; Halary, J. L.; Monnerie, L.; Fetters, L. J. *Macromolecules* **1994**, *27*, 3370.
(53) Bates, F. S.; Wignall, G. D.; Koehler, W. *Phys. Rev. Lett.* **1985**, *55*, 2425. Bates, F. S.; Wignall, G. D. *Phys. Rev. Lett.* **1986**, *57*, 1429.
(54) Gehlsen, M. P.; Rosedale, J. H.; Bates, F. S.; Wignall, G. D.; Hansen, L.; Almdal, K. *Phys. Rev. Lett.* **1992**, *68*, 2452.
(55) Honnell, K. G.; Curro, J. G.; Schweizer, K. S. *Macromolecules* **1990**, *23*, 3496.
(56) Curro, J. G. *Macromolecules* **1994**, *27*, 4665.
(57) Hammouda, B.; Bauer, B. J.; Russell, T. P. *Macromolecules* **1994**, *27*, 2357.
(58) Smith, G. D.; Jaffe, R. L.; Yoon, D. Y. *Macromolecules* **1994**, *27*, 3166.

MA9450492